Dysregulated autophagy in the RPE is associated with increased susceptibility to oxidative stress and AMD

Sayak K Mitter,[1,2,†] Chunjuan Song,[2,†] Xiaoping Qi,[1] Haoyu Mao,[3] Haripriya Rao,[2] Debra Akin,[2] Alfred Lewin,[3] Maria Grant,[1] William Dunn, Jr,[2] Jindong Ding,[4] Catherine Bowes Rickman,[4] and Michael Boulton[1,*]

[1]Department of Ophthalmology; Indiana University School of Medicine; Indianapolis, IN USA; [2]Department of Anatomy and Cell Biology; University of Florida; Gainesville, FL USA; [3]Department of Molecular Genetics and Microbiology; University of Florida; Gainesville, FL USA; [4]Departments of Ophthalmology and of Cell Biology; Duke University Medical Center; Durham, NC USA

[†]These authors equally contributed to this work.

Autophagic dysregulation has been suggested in a broad range of neurodegenerative diseases including age-related macular degeneration (AMD). To test whether the autophagy pathway plays a critical role to protect retinal pigmented epithelial (RPE) cells against oxidative stress, we exposed ARPE-19 and primary cultured human RPE cells to both acute (3 and 24 h) and chronic (14 d) oxidative stress and monitored autophagy by western blot, PCR, and autophagosome counts in the presence or absence of autophagy modulators. Acute oxidative stress led to a marked increase in autophagy in the RPE, whereas autophagy was reduced under chronic oxidative stress. Upregulation of autophagy by rapamycin decreased oxidative stress-induced generation of reactive oxygen species (ROS), whereas inhibition of autophagy by 3-methyladenine (3-MA) or by knockdown of ATG7 or BECN1 increased ROS generation, exacerbated oxidative stress-induced reduction of mitochondrial activity, reduced cell viability, and increased lipofuscin. Examination of control human donor specimens and mice demonstrated an age-related increase in autophagosome numbers and expression of autophagy proteins. However, autophagy proteins, autophagosomes, and autophagy flux were significantly reduced in tissue from human donor AMD eyes and 2 animal models of AMD. In conclusion, our data confirm that autophagy plays an important role in protection of the RPE against oxidative stress and lipofuscin accumulation and that impairment of autophagy is likely to exacerbate oxidative stress and contribute to the pathogenesis of AMD.

Introduction

There are 2 major pathways for the degradation of cellular components in eukaryotic cells: the ubiquitin-proteasome system (UPS) and autophagy-lysosome pathway.[1,2] Autophagy can be subdivided into chaperone mediated, microautophagy, and macroautophagy, but it is only the latter that has the capacity for degrading entire organelles and large protein aggregates.[3-5] Autophagy is a multistep process whereby the cytoplasmic cargo is sequestered by double-membrane autophagosomes, which fuse with lysosomes resulting in the cargo being degraded.[1,2,5] In most cells autophagy occurs at basal levels to remove damaged organelles and protein aggregates as part of a cellular repair process. However, in response to oxidative stress, autophagy is significantly increased in an attempt to remove oxidatively damaged organelles such as mitochondria.[6] There is accumulating evidence linking autophagic impairment with a range of age-related neurodegenerative diseases including age-related macular degeneration.[7-9]

The retinal pigmented epithelium (RPE) is a monolayer of pigmented cells located between the neural retina and choroid. The RPE is essential for the maintenance and survival of overlying photoreceptor cells as it performs a number of critical

functions, i.e. formation of the outer blood retinal barrier, transepithelial transport, maintenance of the retinoid cycle, phagocytosis, and degradation of photoreceptor outer segment tips, and protection against light and oxidative stress.[10] The RPE is particularly susceptible to oxidative damage since it is extremely metabolically active, highly oxygenated, and exposed to photosensitizers such as the age-pigment, lipofuscin.[10] This sensitivity leads to a variety of age-related changes that culminate in reduced RPE function and increased susceptibility to cell death. Oxidative stress is a recognized risk factor for AMD in which changes to the RPE and areas of focal loss result in photoreceptor degeneration and loss of central vision.[11] Increased mitochondrial damage and generation of reactive oxygen species (ROS) are associated with AMD, suggesting that damaged mitochondria and other oxidatively modified components are not efficiently removed by the aged-RPE cell.[11,12] Autophagy is especially crucial in the maintenance of homeostasis of the RPE since these cells are exposed to sustained oxidative stress.[6] A number of studies have reported that autophagy occurs in the RPE.[13-16] However, insufficient digestion due to impaired autophagy or lysosomal degradation in the RPE is reported to lead to an accumulation of damaged organelles, toxic proteins including lipofuscin, and extracellular drusen deposits, all of which can contribute to RPE dysfunction or death and have been associated with the pathogenesis of AMD.[7,10,17] To better understand the role of the autophagy-lysosome pathway for RPE homeostasis, aging, and AMD, we studied the autophagic process and the cellular and molecular pathways under oxidative stress. This study shows that acute exposure to oxidative stress increases autophagy while chronic oxidative exposure reduces autophagy. We observed that the autophagic clearance system is significantly enhanced in both early-onset AMD mouse models and AMD patient samples, but it was reduced in late AMD. In addition, we observed that downregulating the autophagic pathway rendered the RPE more susceptible to oxidative stress while increased autophagic flux protected the RPE from oxidative damage.

Results

Acute H_2O_2 treatment increases autophagy flux in the RPE

We first wished to determine the effect of a single exposure to sublethal oxidative stress on autophagy in RPE cells. Exposure of ARPE-19 cells to either 200 or 400 μM H_2O_2 resulted in transient oxidative damage as seen by an increase in carbonylated protein content but did not result in loss of cell viability (**Fig. 1A and B**). We next examined the effects of H_2O_2 exposure on the autophagic pathway in RPE cells. We first detected the autophagic response by determining the change in expression of MAP1LC3/ LC3 (microtubule-associated protein 1 light chain 3). LC3-I, a cytosolic protein, undergoes lipidation to form LC3-II, which is involved in formation of the autophagosome.[18] The ratio of LC3-II to LC3-I is widely regarded as a critical indicator of autophagic activation. Western blot analysis with an anti-LC3 antibody showed that LC3-II and the ratio of LC3-II/-I was significantly increased at 3 h after treatment of ARPE-19 cells

with H_2O_2 and that the increase was greatest at the highest dose of H_2O_2 tested (**Fig. 1C**), thus demonstrating that acute exposure to H_2O_2 leads to autophagic activation. By 24 h the autophagic response was dampened and only apparent at 400 μM H_2O_2. Blocking autophagosome-lysosome fusion with bafilomycin A_1, which prevents autophagosomal cargo degradation, can be used to rule out the possibility that the accumulation of LC3-II is due to lysosomal disruption.[18] We show that H_2O_2 exposure also increased LC3-II protein level and the ratio of LC3-II/-I even when the lysosomes were disturbed by bafilomycin A_1, confirming that LC3-II accumulation was not due to impaired lysosomal degradation (**Fig. 1C**). We also confirmed that the autophagic response was not specific to the ARPE-19 cell line since the LC3-II/-I ratio was similar in hRPE cells exposed to H_2O_2 (**Fig. 1D**). In both cell types, the autophagic induction was more robust at 3 h following H_2O_2 exposure compared to 24 h, suggesting that autophagy was reduced as oxidatively damaged material was removed. Formation of autophagosome puncta containing LC3 has been regarded as a hallmark of autophagic activation.[18] To evaluate the formation of autophagosomes we traced the formation of autophagic puncta at different time points (3 or 24 h) after oxidative challenge by immunostaining for LC3. In control ARPE-19 cells, LC3 fluorescence was predominantly dispersed throughout the cytoplasm with only a few baseline autophagosomes present while, in contrast, in H_2O_2-treated cells, the number of characteristic punctate fluorescent autophagosomes significantly increased (**Fig. 1E**). To assess the expression levels of some key proteins we evaluated the levels of BECN1, ATG7, and ATG9 at 3 h and 24 h by protein gel blot. However, no significant changes were observed for these proteins at these time-points (**Fig. 2**).

To confirm that the enhancement of autophagic flux is a common event in the RPE in response to acute oxidative stress, we examined the autophagic response following treatment with rotenone, which is an inhibitor of mitochondria complex I, and leads to increased superoxide generation.[19] ARPE-19 cells treated with 1 or 10 μM rotenone for 24 h did not demonstrate any significant loss of cell viability by the crystal violet assay but did show a small (<14 %), but significant, reduction in mitochondrial respiration (**Fig. 3A**). ARPE-19 cells treated with rotenone demonstrated a significant increase in LC3-II expression and the ratio of LC3-II/-I (**Fig. 3B**). A similar response was observed when cells were immunostained for endogenous LC3, with an increased number of autophagosomes in rotenone-treated cells compared to untreated control (**Fig. 3C**). Cell starvation, a common positive control in autophagy experiments, showed a dramatic increase in the LC3-II/-I ratio (**Fig. 3B**). Western blot analysis for expression of the autophagy proteins ATG7, ATG9, and BECN1 (**Fig. 3D**) revealed similar results to that achieved with H_2O_2, in that there were no significant changes in protein levels.

Chronic H_2O_2 treatment reduces autophagic flux and the expression of autophagic factors in the RPE

We next investigated whether chronic oxidative stress, which has been implicated in the pathogenesis of AMD and other neurogenerative diseases,[11,20] affected autophagy in cultured RPE

cells in a similar fashion to a single acute exposure. ARPE-19 cells received repeated exposure to H_2O_2 (200 µM or 400 µM) every 24 h for up to 14 d. The level of damage as measured by protein carbonyl content in cells challenged by oxidative stress continued to be higher than in untreated control (**Fig. 4A**), but was lower than that for acute exposure (**Fig. 1B**). Chronic stress with 200 or 400 µM H_2O_2 did not lead to a loss in cell viability (**Fig. 4B**) or a change in cell morphology (**Fig. 4C**), but cell death was observed at 600 µM and higher (data not shown). Interestingly, we noticed a significant reduction in mitochondrial respiration for ARPE-19 cells at the 14 d time-point (**Fig. 4C**). Western blot analysis demonstrated that the ratio of LC3-II/-I dramatically decreased in ARPE-19 cells upon prolonged exposure to H_2O_2 (**Fig. 4D**). A similar response was observed for hRPE cells exposed to oxidative stress (**Fig. 4E**) and treatment of both cell types with bafilomycin A_1 led to an increase in LC3-II. We next assessed expression of key autophagic proteins ATG7, ATG9, and BECN1. The levels of BECN1 and ATG9 were significantly reduced in ARPE-19 cells treated with chronic oxidative stress at all concentrations while the level of ATG7 was reduced at 400 µM hydrogen peroxide only (**Fig. 4F**). Together, these results demonstrate that repeated exposure to H_2O_2 caused a reduction in autophagic flux in RPE cells.

Modulation of autophagy regulates oxidative stress-induced ROS generation, mitochondria activity, and cell viability in ARPE-19 cells

To further examine the role of autophagy in oxidative stress-induced cell toxicity in RPE cells, we assessed the cellular response to exogenous H_2O_2 after stimulation or inhibition of autophagy by rapamycin or 3-methyladenine (3MA), respectively.

We first confirmed that 3-MA inhibited autophagy whereas rapamycin promoted autophagy under oxidative stress by counting the number of LC3-positive puncta/autophagosomes (**Fig. 5A**). Moreover the mitochondrial activity measured by the MTT assay was significantly reduced in 3-MA and H_2O_2 co-treated cells compared to cell treated with H_2O_2 alone (**Fig. 5B**). Treatment with rapamycin protected ARPE-19 cells from a lethal dose of H_2O_2 (1.5 mM), whereas 3-MA treated cells showed decreased viability in response to H_2O_2

Figure 1. Acute H_2O_2 treatment increases autophagy flux in the RPE. ARPE-19 (**A, B, C, E**) and hRPE (**D**) cells were subjected to sublethal levels of H_2O_2 (200 or 400 µM) for up to 24 h. (**A**) Protein carbonyl levels and (**B**) cell viability and mitochondrial respiration following exposure to H_2O_2. (**C, D**) Autophagic flux was monitored in the presence or absence of bafilomycin A_1 (Baf A_1; 75 nM) by LC3-II/-I conversion with anti-LC3 antibody. Anti-ACTB antibody was used as an internal control. A representative protein gel blot is shown together with densitometric quantification of the LC3-II/-I ratio from a mean of 3 experiments. Differences between groups were considered statistically significant when $P < 0.05$. (**E**) Autophagosome counts in ARPE-19 cells were obtained following immunostaining with LC3 antibody to identify autophagic puncta. A representative set of photomicrographs is shown for control cells and those exposed to H_2O_2. Autophagosome numbers were counted in a minimum of 3 experiments and statistical significance between the control group and each treatment group was determined by ANOVA. Differences between groups were considered statistically significant when $P < 0.05$.

(**Fig. 5C**). To confirm that the loss of cell viability and increased ROS production was not due to nonspecific effects of 3-MA, we used lentiviral shRNA to knock down *BECN1* and *ATG7* expression in the ARPE-19 cells (**Fig. 5D**). The loss of autophagic
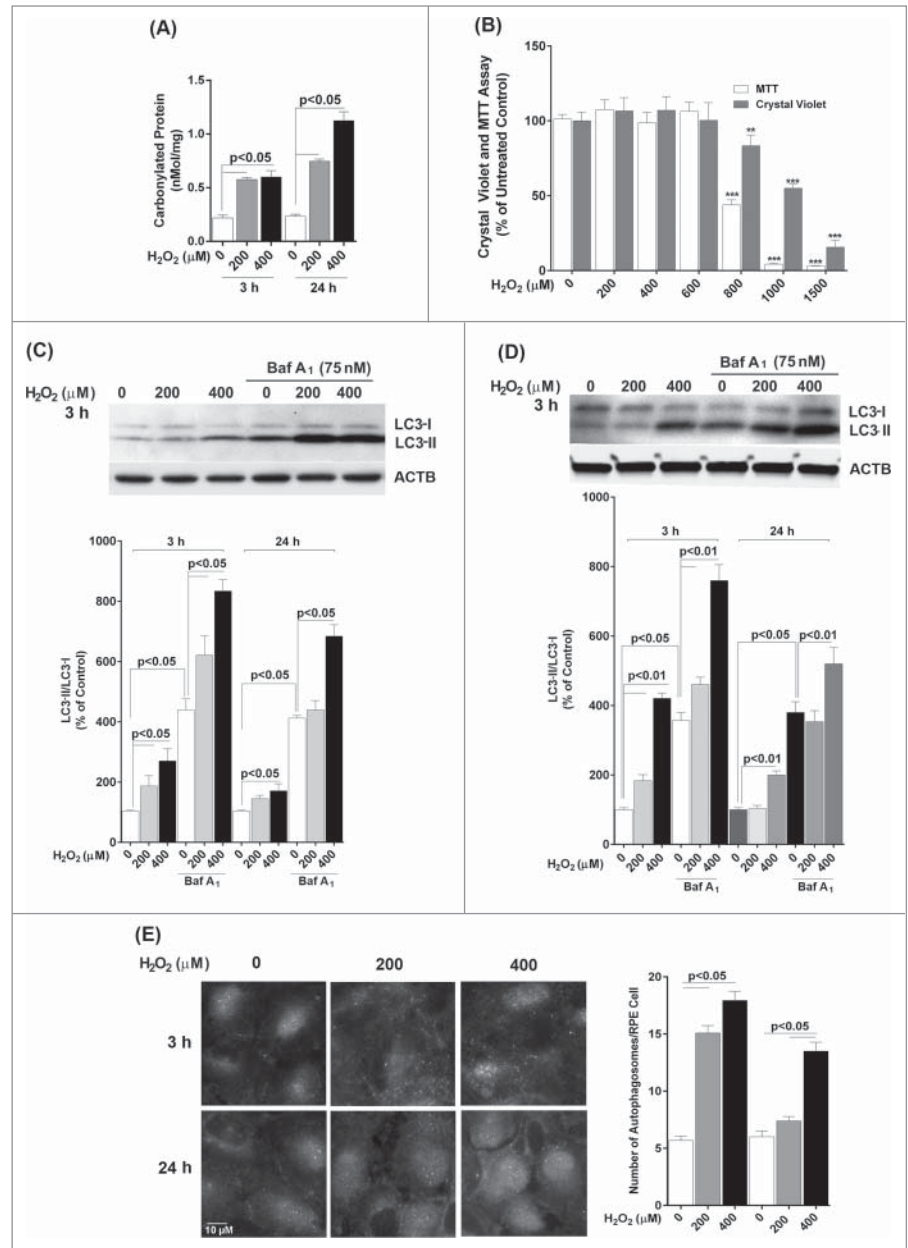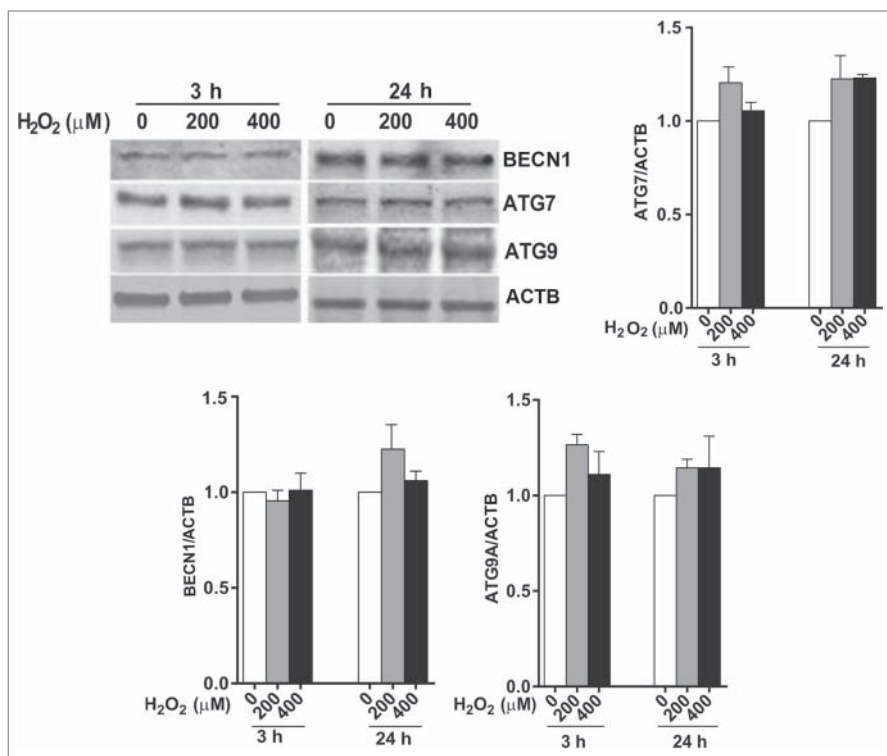
Figure 2. The effect of H_2O_2 on the expression of the autophagy-related proteins BECN1, ATG7, and ATG9 in ARPE-19 cells was determined by western blot. ACTB was used as an internal control. A representative protein gel blot is shown together with densitometric quantification from a mean of 3 experiments. Differences between groups were considered statistically significant when $P < 0.05$.

activity was confirmed by fluorescent autophagosome counting and LC3 lipidation (data not shown). As expected, both gene knockdowns caused RPE cells to show higher susceptibility to H_2O_2 exposure (**Fig. 5E**).

A reduction in mitochondrial membrane potential (MMP) is frequently observed in cells under oxidative stress.[21] We therefore wanted to evaluate whether autophagy in the RPE protects against loss of MMP. We assessed MMP using JC-1 dye and measuring the red/green ratio. A decrease in MMP in ARPE-19 cells was observed 3 h following exposure to 200 and 400 μM H_2O_2 (**Fig. 6A**), which was not apparent at 24 h (data not shown), indicating the ability of the RPE mitochondria to recover from acute oxidative stress over a longer 24-h period. Pre-treatment with rapamycin rescued the cells from the loss of MMP (**Fig. 6A**). We next investigated whether a similar response was obtained if ARPE-19 cells were treated with rotenone as the stressor. As expected rotenone prevented this decrease in MMP (**Fig. 6B and C**). To further test whether inhibition of basal autophagy sensitizes the mitochondria to oxidative stress, we compared the MMP of stable *ATG7* shRNA-transfected ARPE-19 cells to scrambled shRNA transfected cells. *ATG7* knockdown itself did not affect MMP. However, MMP was significantly decreased in *ATG7* knockdown ARPE-19 cells 24 h after exposure to 200 and 400 μM H_2O_2 (**Fig. 6D and E**). Interestingly,

loss of MMP was also observed to occur at lower concentrations of H_2O_2 indicating that inhibiting autophagy increased susceptibility to mitochondrial damage. Although at 24 h we saw a recovery trend of MMP in ARPE-19 cells treated with 200 and 400 μM H_2O_2 (data not shown), chronic exposure showed dramatic reduction of MMP (**Fig. 6F**).

Glutathione (GSH) is established as a protective cellular component against oxidative damage caused by ROS. We have previously shown that oxidative stress with H_2O_2 reduces the ratio of reduced to oxidized glutathione (GSH:GSSG) in ARPE-19 cells.[22] We therefore evaluated whether the GSH:GSSG ratios are modulated by autophagy in ARPE-19 cells. Rapamycin treatment did not increase the GSH:GSSG ratio in untreated cells (**Fig. 6G**). However, the decrease in GSH:GSSG ratio following H_2O_2 treatment was attenuated when cells were treated with rapamycin. In order to verify if changes in mitochondrial density are associated with changes in mitochondrial respiration and ROS generation in ARPE-19 cells, we used MitoTracker Green dye to stain the mitochondria and measured the fluorescence intensity in rapamycin-treated cells by flow cytometry. There was no significant difference between rapamycin-treated and untreated cells (**Fig. 6H**) indicating that rapamycin did not cause significant changes to the overall mitochondrial mass.

Exposure of ARPE-19 cells to chronic H_2O_2 (200 μM for up to 14 d) resulted in an increase in ROS generation, which was increased by 30% in RPE cells treated with both H_2O_2 and 3-MA compared to H_2O_2-treated cells (**Fig. 7A**). Moreover, chronic treatment with H_2O_2 together with the autophagy inhibitor 3-MA significantly reduced mitochondria respiration compared to H_2O_2 treatment alone (**Fig. 7B**).

Excessive lipofuscin accumulation in the RPE has a strong association with the pathogenesis of AMD.[17] *In vivo*, RPE lipofuscin is derived from the incomplete lysosomal degradation of phagocytosed photoreceptor outer segments and damaged intracellular organelles.[17] We found that treatment of RPE cells with 3-MA or leupeptin to block the autophagic pathway resulted in an increase in lipofuscin formation over baseline, whereas treatment with rapamycin to enhance autophagy caused a small, but significant, reduction in the baseline level of autofluorescence (**Fig. 7C**). Since lipofuscin formation in the RPE is a byproduct of photoreceptor phagocytosis we also examined whether modulating autophagy affected the accumulation of lipofuscin after feeding the RPE cells with photoreceptor outer segments. Treatment with rapamycin reduced autofluorescence by >20 % in cells fed with photoreceptor outer segments, but both 3-MA and
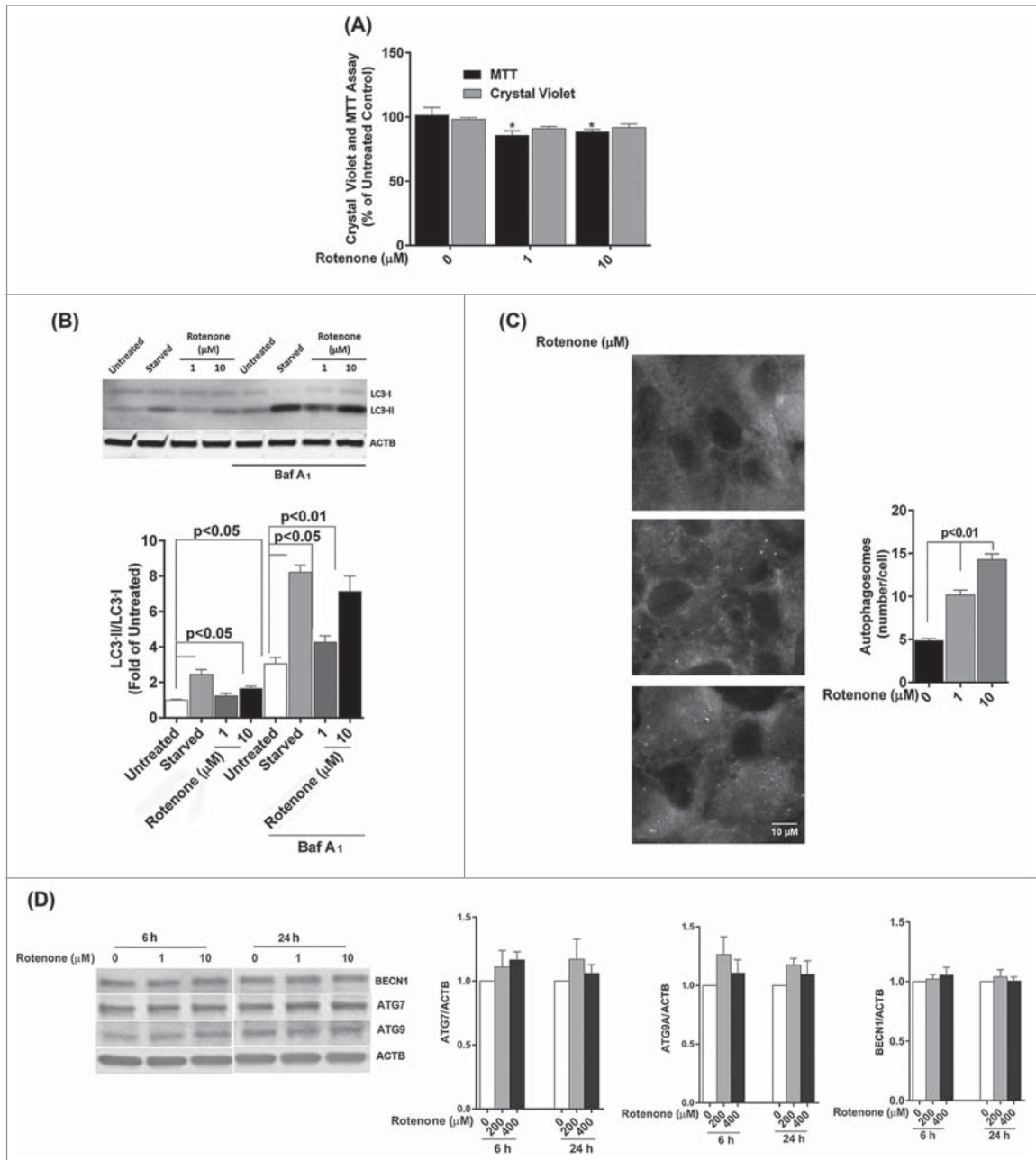
Figure 3. Acute rotenone treatment increases autophagy flux in the RPE. ARPE-19 cells were exposed to 1 or 10 μM rotenone for 6 or 24 h. (**A**) Cell viability and mitochondrial respiration following exposure to rotenone. (**B**) Autophagic flux was monitored by LC3-II/-I conversion using western blot with anti-LC3 antibody. ACTB was used as an internal control. A representative protein gel blot is shown together with densitometric quantification of the LC3-II/-I ratio from a mean of 3 experiments. Differences between groups were considered statistically significant when $P < 0.05$. (**C**) Autophagosome counts in ARPE-19 cells exposed to 0, 1, or 10 uM rotenone for 24 h were obtained following immunostaining with LC3 antibody to identify autophagic puncta. Statistical significance between the control group and each treatment group was determined by ANOVA. (**D**) The effect of rotenone on the expression of the autophagy-related proteins BECN1, ATG7, and ATG9 was determined by western blot. ACTB was used as an internal control. A representative protein gel blot is shown together with densitometric quantification from a mean of 3 experiments. Differences between groups were considered statistically significant when $P < 0.05$.

leupeptin enhanced lipofuscin accumulation (**Fig. 7D**) suggesting a crosstalk between autophagy and phagocytosis. These observations demonstrate that autophagy is an adaptive early response to oxidative stress that reduces cytotoxicity and lipofuscin accumulation in ROS-challenged RPE cells.

Autophagy increases in aging and AMD

We next wanted to evaluate how autophagy changes as a function of age as well as in AMD using 2 mouse models of AMD and human donor specimens from AMD patients and age-matched controls (**Fig. 8A-E, Fig. 9A-C**). Increasing age in both
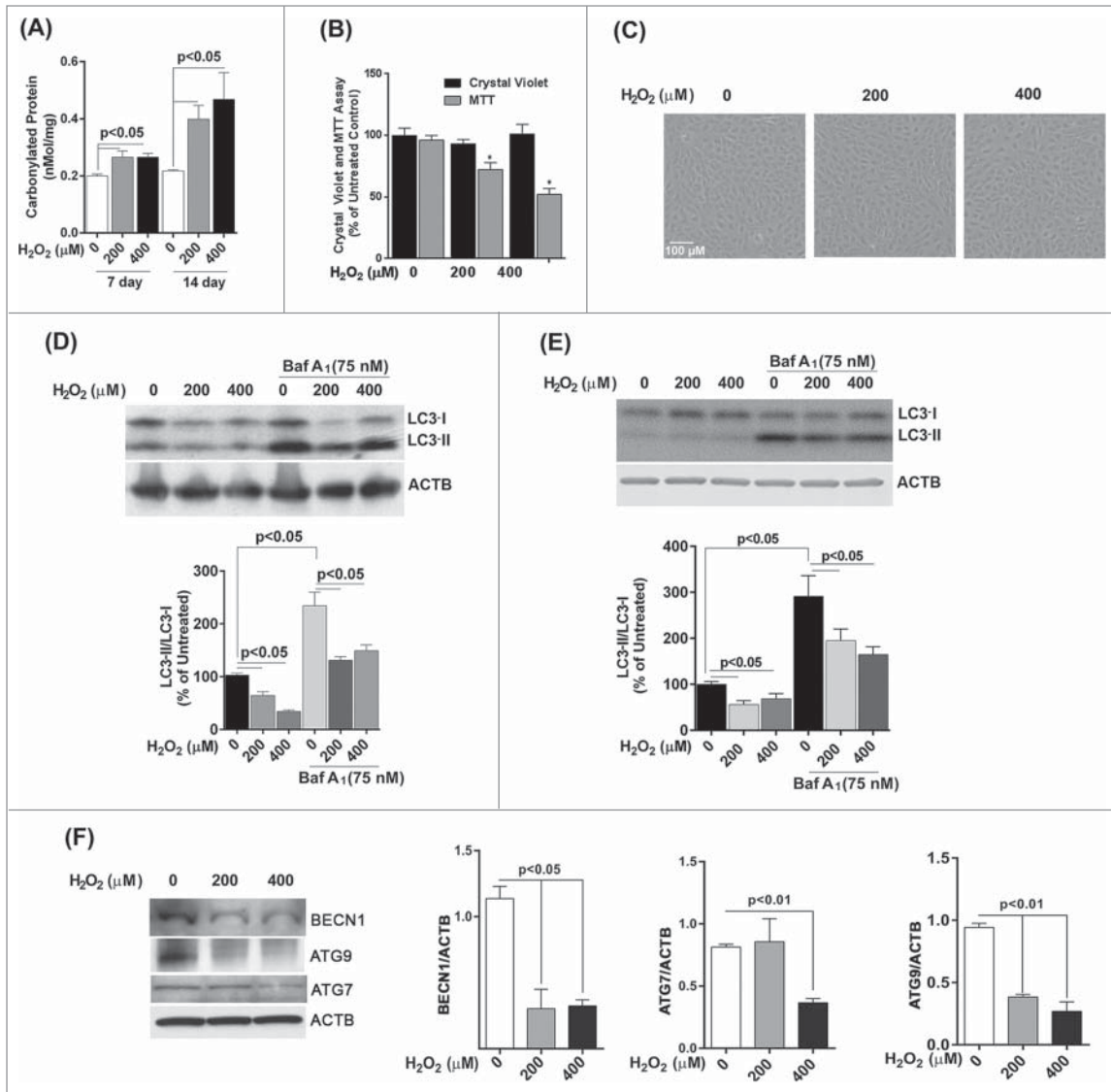
Figure 4. Chronic exposure to hydrogen peroxide reduces autophagic response in the RPE. ARPE-19 (**A–D, F**) and hRPE cells (**E**) were treated with 200 or 400 μM H_2O_2 daily for 14 d. Control cells received vehicle alone. (**A**) Protein carbonyl levels and cell viability following exposure to H_2O_2. (**B**) Cell viability and mitochondrial respiration following exposure to H_2O_2. (**C**) Phase contrast images of ARPE-19 cells either untreated or exposed daily to H_2O_2. Scale bar: 100 μm. (**D,E**) Autophagic flux was monitored in the presence or absence of bafilomycin A_1 (Baf A_1; 75 nM) by LC3-II/-I conversion with anti-LC3 antibody. ACTB was used as an internal control. Representative western blots are shown together with densitometric quantification of the LC3-II/-I ratio from a mean of 3 experiments, Differences between groups were considered statistically significant when $P < 0.05$. (**F**) The effect of H_2O_2 on the expression of the autophagy-related proteins BECN1, ATG7, and ATG9 was determined by protein gel blot. ACTB was used as an internal control. A representative western blot is shown together with densitometric quantification from a mean of 3 experiments. Differences between groups were considered statistically significant when $P < 0.05$.

C57BL6 mice and humans resulted in a greater than 100% increase in the number of autophagosomes in the RPE (**Fig. 8C and 9C**). We elected to use 2 complementary and well-characterized mouse models of AMD for this study; the *Sod2* knockdown model[23] and the *APOE4*-HFC model (aged over 14 mo and fed an HFC diet for 2 mo)[24] to investigate the spatial and temporal changes in the expression levels of autophagy proteins. We noticed that the expression of LC3, ATG7, and ATG9 was dramatically increased in the retina 1 mo after *Sod2* knockdown compared to control. Increased expression of these autophagy

proteins was observed in all retinal layers including the RPE. However, at later time-points, with more advanced AMD phenotype, the expression of these proteins was reduced suggesting that the autophagic response is increased in the early stages of the disease in this model, but that at the later stages autophagy may be impaired (**Fig. 8A**). Similarly, in the *APOE4*-HFC model we noticed an increase in the levels of LC3 and ATG7 as well as ATG9A across the retina, but most predominantly in the RPE for ATG7 (**Fig. 8B**). The fractional volumes of both autophagosomes and autolysosomes in the RPE were measured using
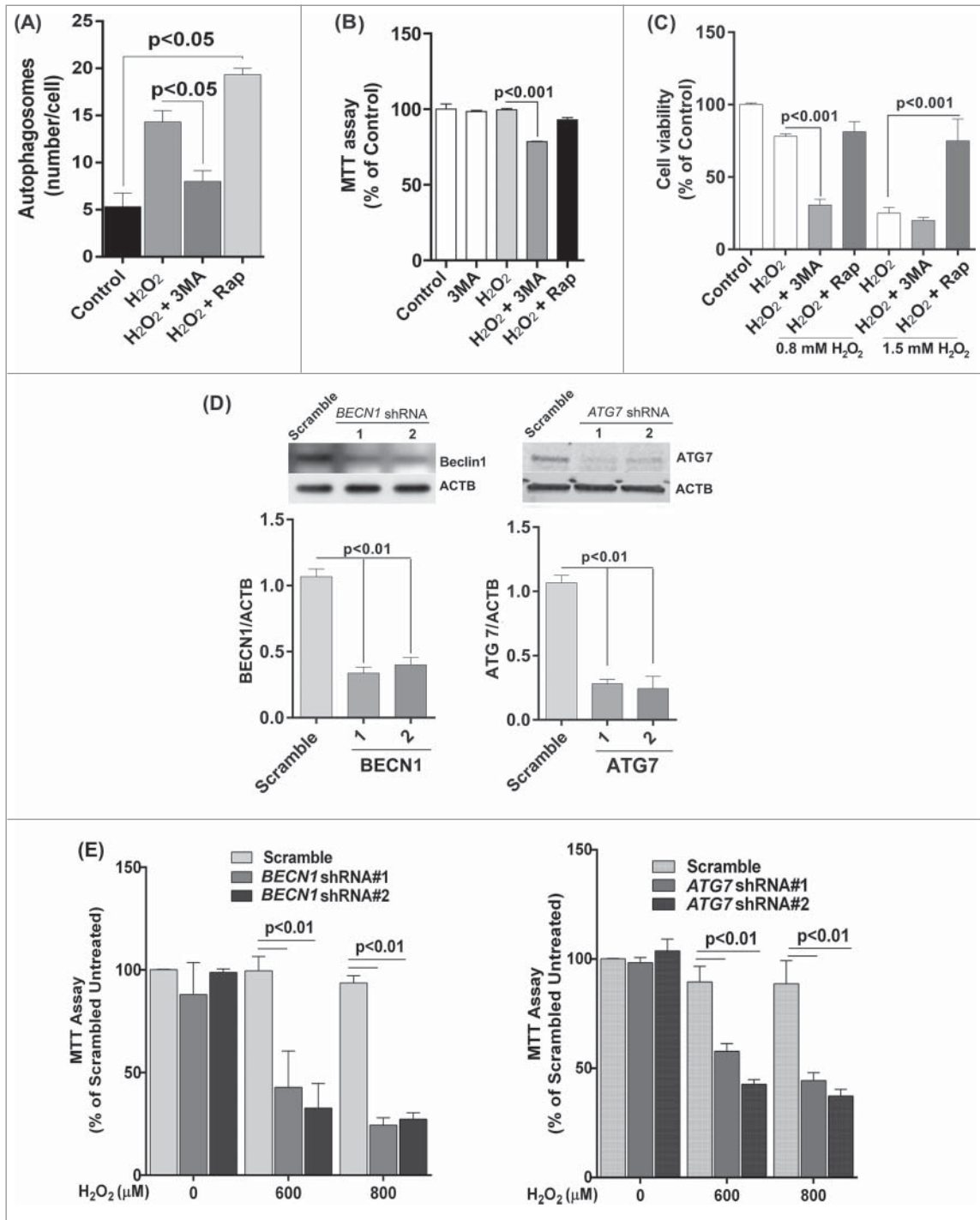
Figure 5. Reduced autophagy renders ARPE-19 cells more susceptible to oxidative stress while increased autophagy protects cells against oxidative stress. (**A**) Autophagosome counts in ARPE-19 cells treated for 12 h with 3-MA (10 mM) or rapamycin (100 nM) and treated with H_2O_2 (400 μM) for 3 h were obtained following immunostaining with LC3 antibody to identify autophagic puncta. (**B**) ARPE-19 cells were pretreated for 12 h with 3-MA (10 mM) or rapamycin (100 nM) and treated with H_2O_2 (400 μM) for 3 h after which mitochondrial respiratory activity was determined using the MTT assay. Differences between means were considered statistically significant from 4 independent experiments when $P < 0.05$ using one-way ANOVA. (**C**) The crystal violet assay was performed on 3-MA and rapamycin pretreated RPE cells and subsequently exposed to 0.8 and 1.5 mM H_2O_2. Differences between means were considered statistically significant from 4 independent experiments when $P < 0.05$ using one-way ANOVA. (**D**) BECN1 and ATG7 knockdown by lentiviral shRNAs in RPE was confirmed by protein gel blot. Knockdown was considered statistically significant when $P < 0.01$ from at least 3 independent experiments (**E**) The MTT assay was performed on ARPE-19 cells with BECN1 or ATG7 knockdown to assess the cell viability in response to increasing concentrations of H_2O_2. Differences between means were considered statistically significant from 4 independent experiments when $P < 0.05$ or 0.01 using one-way ANOVA.
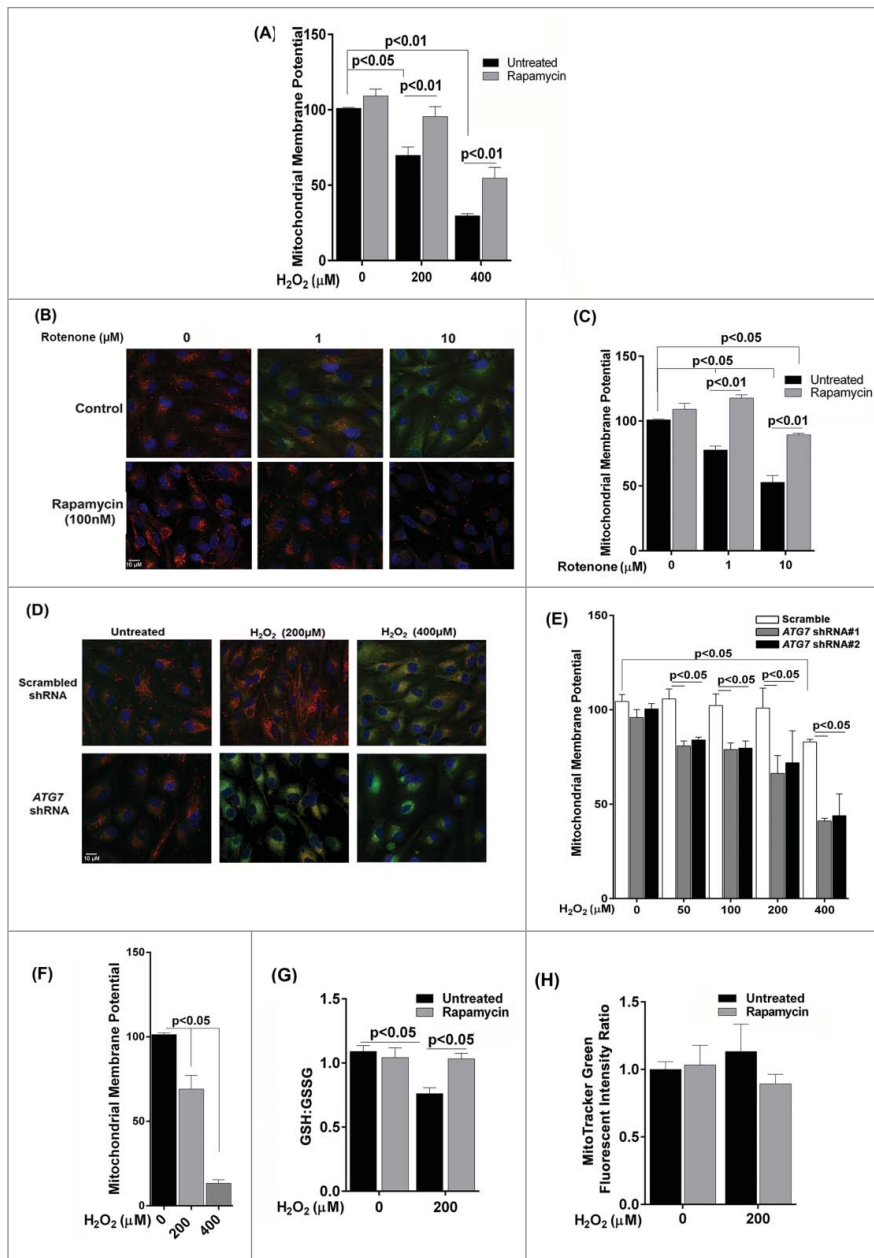
Figure 6. The effect of oxidative stress on mitochondrial membrane potential and glutathione levels in ARPE-19 cells. (**A**) Cells were pretreated with rapamycin for 3 h and then exposed to H_2O_2 (200 and 400 μM) for 3 h. Cells were assessed for mitochondrial membrane potential using the JC-1 dye. (**B, C**) Cells were treated with rotenone (1 and 10 μM) for 24 h and mitochondrial membrane potential determined using the JC-1 dye. (**B**) Representative photomicrographs showing JCI staining. (**C**) Quantitation of JC-1 staining using a fluorometric plate reader. (**D,E**) Stable ATG7 knockdown and scrambled control ARPE-19 cells were treated with H_2O_2 for 24 h and assessed for mitochondrial membrane potential using JC-1 dye. (**D**) Representative photomicrographs showing JC-1 staining. (**E**) Quantification of JC-1 staining using a fluorometric plate reader. (**F**) Mitochondrial membrane potential was measured using JC-1 dye on cells treated for 14 d with H_2O_2 (200 and 400 μM). (**G**) ARPE-19 cells were incubated with H_2O_2 (200 μM) for 24 h and the intracellular GSH:GSSG ratio was determined by the glutathione assay kit. (**H**) Mitochondrial mass was compared following exposure to 200 μM H_2O_2 for 24 h in ARPE-19 cells either pretreated or not treated with rapamycin (100 nM) for 3 h. Data were analyzed using one-way ANOVA and differences between means were considered statistically significant when $P < 0.05$.

morphometric analyses of electron micrographs. Measurement of the fractional volumes of autophagic vacuoles from electron micrographs in the RPE of our AMD animal models demonstrated an increase in both models compared to control although with longer duration of disease in the *Sod2* knockdown model autophagosomes appeared to be reduced compared to early disease (**Fig. 8C and D**). Western blot of autophagy proteins in the RPE/choroid/sclera demonstrated a significant increase in ATG7, ATG9A, and SQSTM1/p62 in the RPE/choroid/sclera, and a small but significant increase in LC3-II/-I (**Fig. 8E**).

Semiquantitative analysis of tissue sections from AMD donors and age-matched controls demonstrated an upregulation of the LC3, ATG7, and ATG9 protein levels in the RPE and also across the retina of the older non-AMD donors when compared to those of the younger non-AMD donors (**Fig. 9A and B**). Age-matched AMD patient retinas showed higher levels of ATG7 and ATG9A, whereas the level of LC3 was reduced in the early AMD stages. However, the late AMD patient retinas exhibited a substantial reduction of the protein levels when compared to the non-AMD and early-AMD specimens. On further comparison of autophagosome fractional volumes in the RPE of donors, we observed that although there is a significant increase in the older donors compared to young, the fractional volume was substantially lower in both early and late AMD donor RPE compared to age-matched controls (**Fig. 9C**).

Discussion

Our study identifies that 1) autophagy is dysregulated in the RPE and neural retina of human AMD specimens and rodent models with an AMD phenotype, 2) oxidative stress significantly alters the autophagic response and 3) increasing autophagy protects against oxidative stress.

Reports on autophagy in the retina include retinal degeneration following acute light exposure[25,26] or retinal ganglion cells following optic nerve transection[27] and regulation of autophagy for RPE cells.[13,14,28-31] Recent studies from our laboratory and others indicate a potential role of autophagy

in lipofuscin accumulation, drusen formation, and AMD pathogenesis.[14,22,31] We found that with aging there seemed to be a dramatic increase in LC3, ATG7, and ATG9 in the RPE as well as other retinal layers of non-AMD human donors and our rodent models. It has been reported that autophagic flux increases during aging due to the ROS-induced intracellular burden of damaged organelles and accumulated macromolecules.[32] Impaired or insufficient autophagy activity in aged cells is implicated in numerous diseases, including inflammatory diseases, neurodegenerative diseases, heart diseases, and cancer.[2,8,9] This increase was also true for the retinas of patients showing signs of early AMD. However, with late-stage AMD the abundance of these proteins seemed to be reduced. These data were corroborated by our analysis of electron micrographs, which demonstrated a decrease in autophagosomes in the diseased state when compared to the age-matched, nondisease donors. Both the mouse models for AMD showed a similar dramatic increase in the earliest disease stages, whereas in the latter stages of the disease the *Sod2* knockdown model showed loss of autophagy markers. There was, however, still a significantly higher number of autophagosomes in the RPE at the 6 mo post-injection stage for this model compared to the nondiseased RPE, whereas 12 mo post-injection, the number appeared to recede. We speculate that this increased autophagosome number at a stage when protein markers have already started to diminish (6 mo post-injection) is a result of reduced lysosomal efficiency to degrade the autophagosomes, which has been implicated in the mechanism of development of AMD.[7,14] While the SOD2/MnSOD disease model gave us the opportunity to observe autophagic phenomena at multiple stages after SOD2 knockdown, the *APOE4*-HFC mouse model of AMD was studied only at a single time-point and showed an increase in the autophagic markers with increased autophagic fractional volumes. A possible explanation for this observation is the requirement of autophagy in lipid catabolism that is encountered in this model due to the inability in maintaining cholesterol homeostasis.[24] It is quite possible that during the 2-mo time period of HFC diet autophagy continues to be stimulated to relieve the lipid burden.[24,33,34] It will be interesting to assess the effect of a longer duration of HFC diet on the *APOE4* model and to measure the levels of the markers in order to completely assess the fate of autophagy. We think that this increase in autophagy is protective since pharmacological upregulation of autophagy in
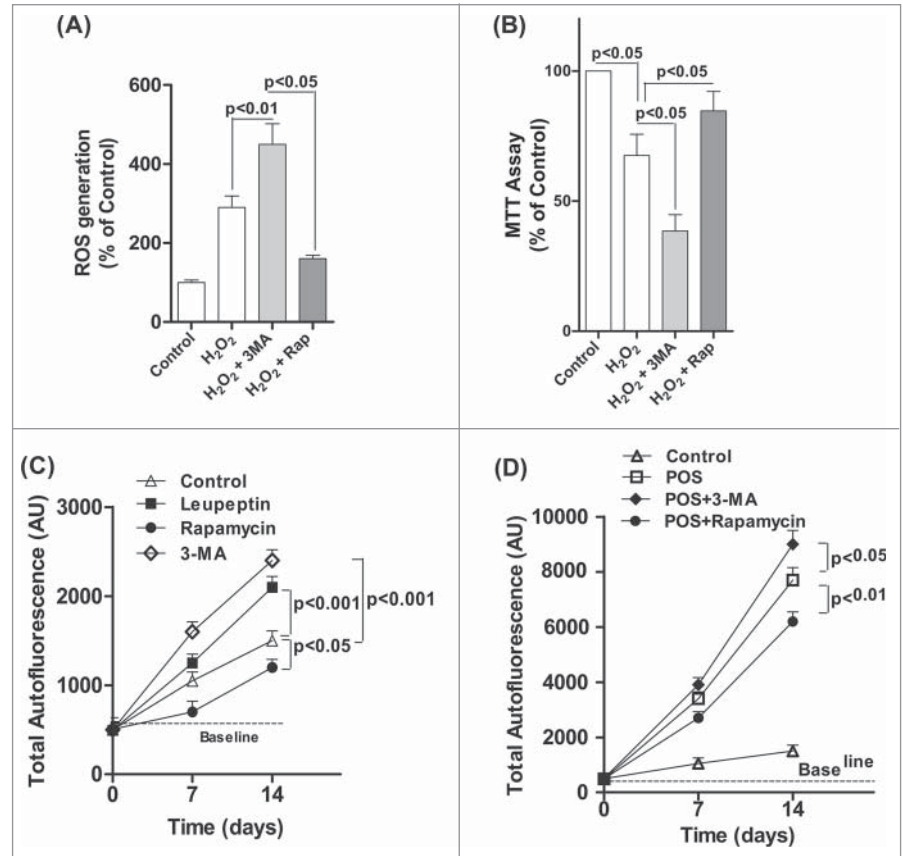

Figure 7. Decreased autophagy increases the generation of reactive oxygen species (ROS) and accumulation of lipofuscin-like granules in the RPE. After daily exposure of ARPE-19 cells to 200 μM H_2O_2 for 14 d 3-MA or rapamycin was added 12 h before assaying for: (**A**) ROS in RPE by the H2DCFDA assay, (**B**) mitochondria respiration using the MTT assay and (**C**) RPE cells maintained in basal medium with daily exposure to leupeptin (100 μM), rapamycin (50 nM), 3-MA (10 mM), or vehicle control for up to 14 d. The accumulation of autofluorescence granules was determined at 7 and 14 d by FACS analysis. (**D**) RPE cells were fed 2×10^7 photoreceptor outer segments (POS)/ml daily either alone or in combination with 3-MA or rapamycin in basal media. Autofluorescent granule accumulation was determined at 7 and 14 d by FACS analysis. For each experiment, differences between means were considered statistically significant from 3 independent experiment when $P < 0.05$.

this model has shown a better survival of RPE (data not shown). Our findings, based on the mouse models and the human disease, suggest that while all mouse models of AMD reproduce the characteristics of the disease, subtle differences remain in the molecular mechanisms that may set them apart from the actual human disease. Based on our current knowledge of aging and the risk factors for AMD we conclude that overall autophagic capacity is increased in aging and early stage AMD to compensate for increasing oxidative stress and damage to intracellular organelles.[7,14] However, we would anticipate that in more advanced AMD, the autophagic system becomes overloaded and is unable to cope with the increase in damaged intracellular organelles and aggregates. Thus, it is likely that changes in autophagy begin as a consequence of aging and AMD but, later the autophagic process becomes impaired and thus contributes to the progression of later-stage AMD.
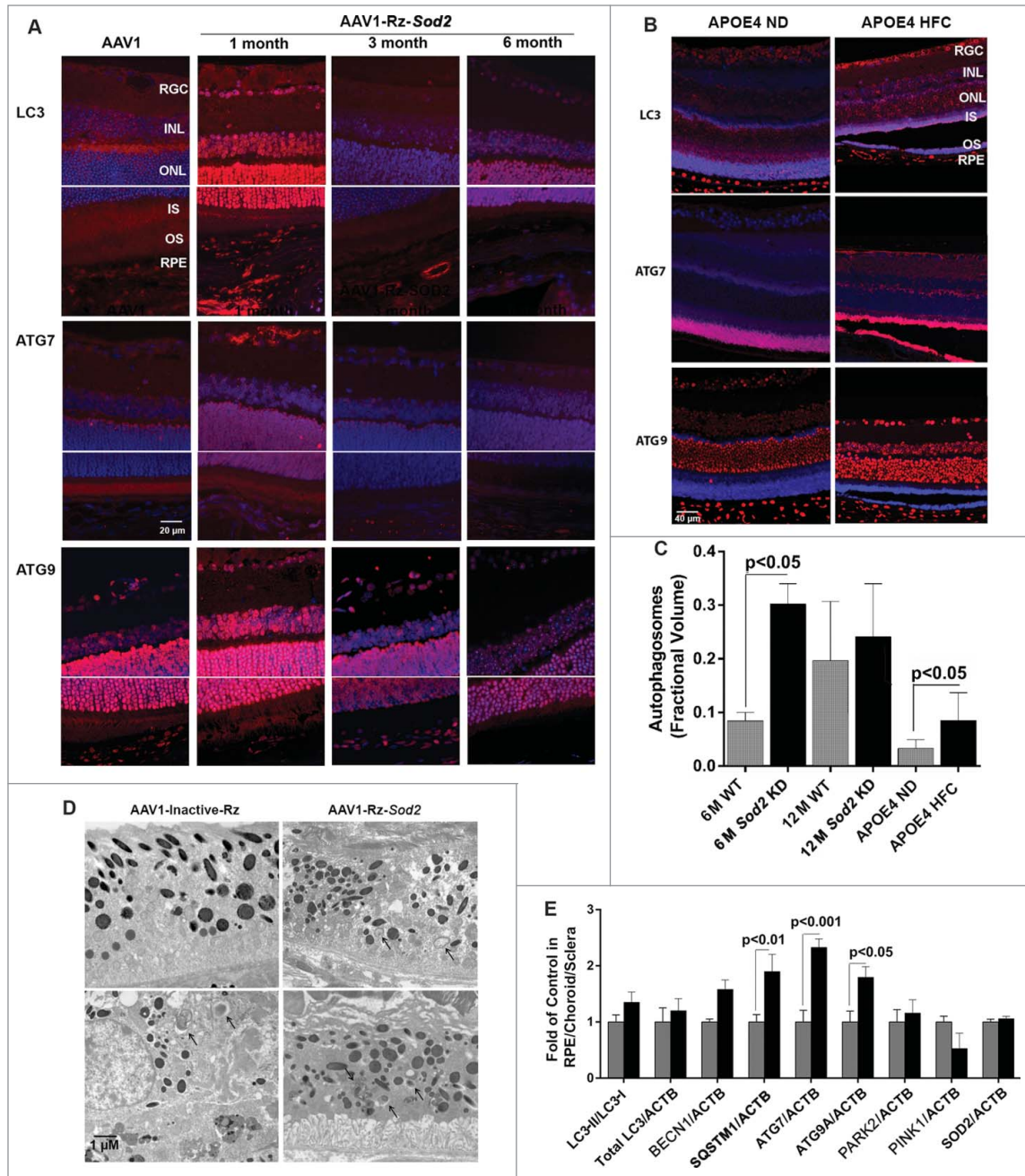
Figure 8. Expression of autophagy proteins and autophagosome volume in 2 rodent models of AMD. (**A**) *Sod2* knockdown in C57BL6 mice was achieved with subretinal AAV1-Rz-*SOD2* (AAV1 containing inactive ribozyme acted as a control). Animals were sacrificed at 1 mo and 3 mo (early AMD) and 6 mo (late AMD) following *Sod2* knockdown (n = 6 per group). (**A**) Retinas were fixed in paraformaldehyde, paraffin embedded, and immunostained for LC3, ATG7 and ATG9 (red), and DAPI was used to visualize the nuclei (blue). Representative photomicrographs are shown for *Sod2* knockdown and control animals. (**B**) *APOE4* mice at the age of 15 mo were fed a high fat, cholesterol-enriched (HFC) diet for a period of 2 mo (n = 6 per group). Age-matched control *APOE4*s were maintained on a normal diet (ND). Retinas were fixed in paraformaldehyde, wax embedded and immunostained for LC3, ATG7, or ATG9 (red), and DAPI was used to visualize the nuclei (blue), Representative photomicrographs are shown for *APOE4*-HFC and *APOE4*-ND control animals. (**C**) Autophagosome fractional volume in the RPE of 6-mo- and 12-mo-old WT mice, *Sod2* knockdown mice at 6 and 12 mo following *Sod2* knockdown and *APOE4* mice on normal (ND) and high fat cholesterol-enriched (HFC) diets (n = 6 per group). (**D**) Representative electron micrographs showing autophagosomes (arrows) in SOD2 knockdown and control animals. Scale bar: 1 μm. (**E**) RPE/choroid/sclera lysates from *APOE4*-HFC (black bars) and *APOE4*-ND (grey bars) mice (n = 6 per group) were assessed for the level of autophagic proteins by western blot and densitometric quantification. Expression was normalized to ACTB as internal control. Differences between means were considered statistically significant when $P < 0.05$.
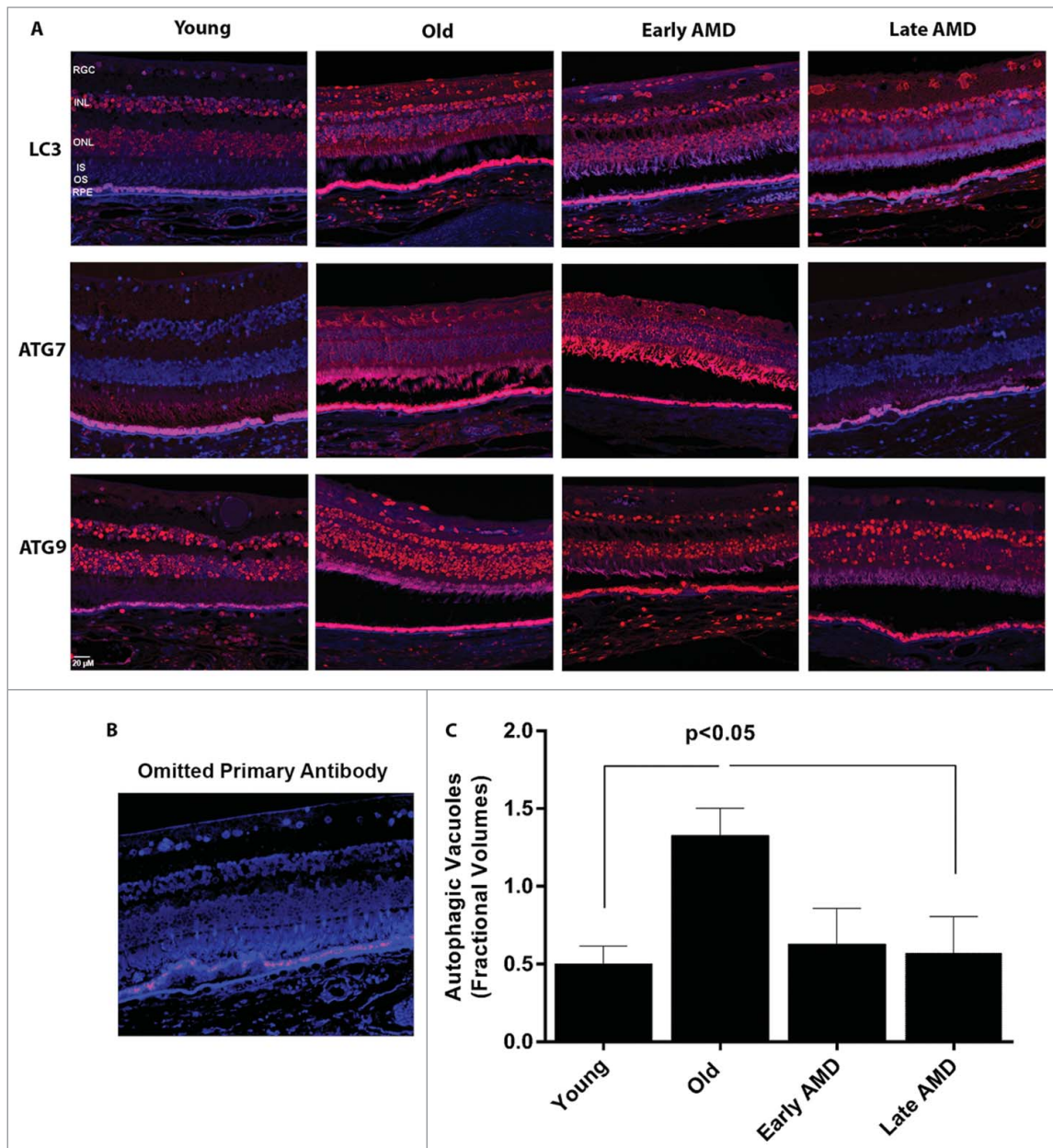
Figure 9. Expression of autophagy proteins and autophagosome volume in human retinas from normal and AMD donors. (**A**) Representative photomicrographs from human donor retinas from young, old, early AMD and late AMD. Retinas were fixed in paraformaldehyde, paraffin embedded, and immunostained for LC3, ATG7 or ATG9 (red), and DAPI was used to visualize the nuclei (blue). Each group had n = 4 specimens for analysis. (**B**) Omission of primary antibody. (**C**) Fractional volumes of autophagosomes in the RPE of human donor retinas from young, old, early AMD, and late AMD determined from electron micrographs (n = 5 per group), $P < 0.05$.

In the present study, we show a dynamic alteration of autophagic flux in cultured RPE cells under oxidative stress: acute (short-term) exposure to oxidative stress increases autophagy activity while, in contrast, chronic (long-term) exposure to oxidative stress induces dramatic autophagy reduction. We have also shown that the activation of autophagy in response to oxidative stress is inhibited by 3-MA, suggesting that the oxidative stress is acting through the class III phosphatidylinositol 3-kinase regulator of autophagy. Furthermore, we systematically demonstrated that increasing autophagic flux protects the RPE from oxidative damage and death whereas downregulating the autophagic pathway renders the RPE cells more susceptible to oxidative stress. Our data suggest that the association between autophagy and oxidative stress may be under 2-way regulation since oxidative stress promotes autophagy and increased autophagy reduces oxidative damage and increases antioxidant capacity thus decreasing the oxidative stimulus. Surprisingly, we showed that autophagy activity increased during aging in the RPE of rodents, which is in

contrast with other tissues in which autophagic activity has been reported to decrease with age.[35] However, we also show that autophagy capacity appears to be reduced by >25 % in AMD donors compared to age-matched controls.

A growing body of evidence from cell culture and animal models indicates that oxidative stress is a key mediator of RPE cell death during aging and the development of age-related macular degeneration.[11,36] Oxidative stress in the RPE is largely derived from (1) ROS generation from mitochondria and photo-oxidation but also partially from NADPH oxidase, and (2) a reduction in the ability to repair/remove oxidatively damaged proteins and organelles.[11,36] In the present study we exposed RPE cells to sublethal concentrations of oxidative stress, but sufficient to induce oxidation of intracellular organelles and macromolecules. Our *in vitro* data on protein carbonylation in ARPE-19 cells is in agreement with values reported previously in these cells[37] and oxidized protein levels at 2 nM/mg protein have been reported in neurons in the substantia nigra, which is within the range in our study.[38] We observed that exposure of naïve cells to a single dose of sublethal oxidative stress resulted in increased autophagy, whereas repeated daily exposure to multiple chronic stress decreased autophagy compared to the control. There is a wide variability in the reported response of cultured RPE cells to H_2O_2 which range from 50 μM to 15 mM[39,40] with Kurz and colleagues reporting that RPE cells are highly resistant to oxidative stress and can survive up to 15 mM H_2O_2.[40] The variation between studies is due to a wide variety of factors: whether the cells are proliferating or confluent, the degree of differentiation, the density of the cells (i.e., the greater the cell number the less effective the oxidative stressor will be),[41] and the culture media. In essence, a proliferating undifferentiated low-density culture will be much more sensitive to H_2O_2 than a confluent, nondividing, differentiated, high-density culture such as we have used. The concentration of H_2O_2 used in this study falls within the published range and has been well validated in publications from this lab.[11,42,43] However, to what extent these H_2O_2 concentrations recapitulate those that occur *in vivo* is unclear due to a paucity of data in this area. Studies suggest that physiological H_2O_2 levels reach around 100 μM in the vitreous[44] and there is reported to be a burst of H_2O_2 generation in the RPE following phagocytosis of photoreceptor outer segments.[45] The increase in autophagy in response to oxidative stress is as expected and reported for other cell types. However, the decrease in autophagy in response to daily chronic oxidative stress can be explained in a number of ways. First, cells located in inherently oxidizing microenvironments use the adaptive response as an important antioxidant defense, and we have previously shown that chronic oxidative stress leads to an increase in CAT/catalase, SOD1/CuZnSOD and glutathione peroxidase activity in the RPE.[42] Thus it is possible that by 14 d exposure to chronic oxidative stress the RPE now shows significantly less oxidative damage and there is reduced need for an autophagic response. This is supported by our observation that protein carbonyl levels are lower in RPE cells exposed to chronic oxidative stress compared to a single exposure. A recent study in retina further supports the idea that macroautophagy may be compromised with age and is compensated for by microautophagy, which can alleviate the load of damaged protein by removing some proteins, but cannot necessarily remove the larger organelles like mitochondria that macroautophagy is specialized to remove.[46] Second, adaptation may lead to a downregulation of autophagy proteins as we observed in this study. It should be emphasized that the H_2O_2 will have degraded in the cultures within about 30 min after application and thus this model represents short bursts of exposure to oxidative stress and probably better reflects the situation in the eye.

Autophagy involves the coordinated activity of more than 30 autophagy-related proteins.[2,5] In the present study, we found that acute exposure to H_2O_2 caused an increase in autophagy proteins while chronic oxidative stress reduced the expression of several key autophagy proteins. BECN1 sits at the center in regulating autophagy by interacting with several cofactors that promote the formation of the BECN1-PIK3C3-PIK3R4 core complex to activate PIK3C3 lipid kinase activity,and induce autophagy.[47] A critical component of the autophagosome, LC3 has been regarded as a primary biochemical marker for autophagy activation. During autophagy, LC3-I, the cytosolic form, is conjugated to phosphatidylethanolamine to form the LC3-phosphatidylethanolamine conjugate (LC3-II), which is then recruited to phagophore membranes; part of the autophagosome-associated pool of LC3-II is then degraded with the cargo in the lysosome. Therefore, monitoring the conversion of LC3-I to LC3-II is indicative of autophagic flux and has been regarded as a reliable autophagy marker.[48] In the RPE, as recent studies suggest, LC3 is implicated in the phagocytic pathway linking it with a noncanonical autophagic degradation pathway.[13] ATG7, an E1 ubiquitin activating-like protein, is involved in the covalent isopeptide linkage of ATG5 and ATG12 to contribute to the elongation of the phagophore membrane. ATG9 is thought to play a role in supply of components for formation of the autophagosomal membrane.[49] Taken together, we found that acute oxidative stress increases autophagic activity, but chronic oxidation decreases autophagy. To assess cumulative autophagic flux induced by oxidative exposure, we used bafilomycin A_1 that prevents autophagosome–lysosome fusion thereby blocking the degradation of LC3-II in the lysosome, and we obtained results in agreement with the 'steady state' experiments (without bafilomycin A_1 co-treatment). While LC3-I accumulation was obvious with rotenone treatment there was no change in the levels of BECN1, ATG7, or ATG9 expression. This may not be unexpected since progression of the autophagy pathway is more dependent on mobilization of autophagy proteins that are constitutively expressed rather than upregulation of these proteins. While the proteins BECN1, ATG7, and ATG9 are critical for the autophagic pathway to function, they are not required to be upregulated for the pathway to be stimulated following acute oxidative stress. However, in the long-term

stress model, these proteins are depleted and this leads to a decrease in autophagy as we have shown in this study.

Numerous studies have reported the role of autophagy in regulating cell fate under stress.[50-52] While suggesting that autophagy may be detrimental to the cell when under stress, many other reports suggest that induction of autophagy is a protective attempt by the cell to evade death under stress conditions that often turn out to be a futile effort under an overwhelmingly challenging environment.[50-52] Although a role in damage vs. protection remains a subject of strong debate, autophagy is considered to be a process that is critical in maintaining cellular function and quality.[2,5] Herein, we also demonstrated that autophagy is implicated in the pathogenesis of AMD. Stimulation of autophagy by rapamycin improved autophagic efficiency and protected RPE cells against cell death exposed to lethal concentrations of H_2O_2. Rapamycin is widely used to stimulate macroautophagy by inhibition of the mechanistic target of rapamycin, MTOR.[53] However, MTOR is a kinase at a key signaling node that integrates information regarding extracellular growth factor stimulation, nutrient availability, and metabolism and thus is not specific for the autophagy pathway.[53] Our western blot and LC3 expression data clearly demonstrate that rapamycin is increasing autophagy but it is possible that rapamycin could also be acting, in part, by modulating metabolism. Inhibiting autophagy either pharmacologically or by inhibiting endogenous expression of key autophagic proteins caused cell viability and mitochondrial activity to be compromised. Furthermore, we show some key features of stressed RPE such as increased buildup of ROS and lipofuscin when autophagy is compromised. Conversely, stimulating the autophagic pathway significantly decreases this accumulation. This finding essentially corroborates reports in the literature that loss of autophagy-lysosomal degradation can contribute to buildup of lipofuscin.[22,29,54,55] Although in our studies we did not witness a change in mitochondrial density by enhancing autophagy with rapamycin, we found that reduction in the intracellular GSH:GSSG ratio after oxidative stress was attenuated by rapamycin suggesting that enhancing autophagy may offer protection to RPE by increasing the antioxidant activity of glutathione.

In summary, we present a novel finding that the low-dose oxidative stress in short-term exposure is able to induce autophagy activation as an early event to prevent oxidative damage to RPE cells, whereas long-term oxidative exposure decreases autophagy and causes cell death. We also show that the autophagy enhancer rapamycin has a protective effect against H_2O_2-induced ROS generation, but the autophagy inhibitor 3-MA renders cells more susceptible to H_2O_2-induced cell toxicity and cell death, indicating the protective role of autophagy in RPE cells under oxidative exposure. It seems most likely that autophagy is a response to increased oxidative stress in AMD and that this activates the autophagy pathway as a protective response. Subsequent impairment of autophagy will then contribute to the progression of AMD through the failure to remove damaged organelles. Upregulating autophagy may offer an alternative therapeutic strategy to slow or halt the progression of AMD by preventing the accumulation of oxidatively damaged material in retinal cells.

Materials and Methods

Materials

The ARPE-19 (ATCC, CRL-2302) and HEK293T (ATCC, CRL-3216) cell lines were obtained as frozen vials and seeded in appropriate tissue culture media. Human donor eyes for cell culture were obtained from NDRI. Hydrogen peroxide (Sigma-Aldrich, 216763–100ML), rotenone (Sigma-Aldrich, R8875), 3-methyladenine (3-MA; Sigma-Aldrich, M9281), rapamycin (Sigma-Aldrich, R0395–1MG), bafilomycin A_1 (Sigma-Aldrich, B1793), thiazolyl blue tetrazolium bromide (MTT; Sigma-Aldrich, M5655), leupeptin (Sigma-Aldrich, 2884), metaphosphoric acid (Sigma-Aldrich, 239275), triethanolamine (Sigma-Aldrich, T58300), 2-vinylpyridine (Sigma-Aldrich, 132292) and Krebs-Henseleit Buffer (Sigma-Aldrich, K3753) were obtained and reconstituted according to the manufacturer's recommendations. DMEM cell culture medium (Cellgro, 10–013-CV) Ham's F10 cell culture medium (Cellgro, 10–070-CV), Opti-MEM reduced serum medium (Invitrogen, 31985070), fetal bovine serum (FBS; Sigma-Aldrich, 26140079), trypsin-EDTA solution (0.05% and 0.25%) (Cellgro, 25–052-Cl and 25–050-CI), TRIzol reagent (Cellgro, 15596–018), Lipofectamine LTX transfection reagent (Invitrogen, 15338–100) and Lipofectamine 2000 transfection reagent (Invitrogen, 11668–027) were purchased from Life Technologies. Two′, 7′-dichlorodihydrofluorescein diacetate (H2DCFDA; EMD Chemicals, 287810–100MG) was obtained and reconstituted according to the manufacturer's recommendations. The Bradford protein assay kit (Bio-Rad Laboratories, 500–0201) was purchased and used following the manufacturer's protocol. The primary antibodies used in this study were rabbit polyclonal antibodies anti-LC3 (Novus Biologicals, NB100–2220), anti-ATG9A (Novus Biologicals, NB110–56893), mouse monoclonal antibodies anti-ACTB (Sigma-Aldrich, A5441), anti-α-tubulin (Sigma-Aldrich, T9026), rabbit polyclonal antibody anti-ATG7 (Sigma-Aldrich, SAB1407006), and mouse monoclonal anti-BECN1/Beclin 1 (BD Biosciences, 312113). Anti-mouse IgG (whole molecule)–peroxidase antibody (Sigma-Aldrich, A9044), anti-rabbit IgG (whole molecule)–peroxidase secondary antibodies (Sigma-Aldrich, A0545) and ECL chemiluminescence kit (Amersham Pharmacia Biotech, RPN2132) were obtained from the indicated sources. IRDye 800-conjugated anti-rabbit (Rockland Labs, 611–132–002) and Alexa Fluor 680 conjugated goat anti-mouse (Invitrogen, A-21058) secondary antibodies were obtained and used for protein gel blotting and immunohistochemistry based on the manufacturer's recommendations. MitoTracker Green dye (Invitrogen, M-7514) and JC-1 dye (Invitrogen, T-3168) were prepared as recommended.

Cell culture and treatment paradigm

Human ARPE-19 cells were grown in Ham's F10 Medium containing 10% FBS at 37°C in a humidified atmosphere containing 5% CO_2/95% air as we have previously described.[42] Primary human RPE was cultured from postmortem human eyes (Age: 16 to 61 y) obtained from NDRI as previously described in Ham's F10 media containing 20% FBS and supplemented with

0.4% glucose (Fisher Scientific, D16–1).[56] Primary cultures were used between 2nd and 4th passage. ARPE-19 cells and primary human RPE cells were grown to confluence on plastic culture dishes and maintained in basal media (Ham's F10 Medium + 2% FBS) for up to 7 d before experimentation to allow the cells to develop a polarized epithelial layer. Cultures were exposed to either 0–400 μM H_2O_2 or 0–10 μM rotenone in basal medium. For "acute" exposure studies cells received a single application of H_2O_2 or rotenone for 6 h and for "chronic" studies cells were exposed to H_2O_2 as indicated daily for 14 d. Selected studies were undertaken in the presence of the autophagy activator rapamycin (100 nM) or the autophagy inhibitor 3-MA (10 mM) for the duration of the experiment. Untreated or vehicle-treated cells were used as controls. For starvation, ARPE-19 cells were incubated with sterile filtered Krebs-Henseleit Buffer supplemented with $CaCl_2$ at 37°C for 3 h.

Western blot analysis

Cells were lysed in RIPA buffer (Thermo Scientific, 89901) containing protease inhibitor (Roche Applied Science, 11873580001). Cell lysates containing equal amounts of protein were loaded in each lane and separated on a 12% SDS-PAGE gel. After separation, proteins were transferred to a nitrocellulose membrane (0.22 μm; Bio-Rad Laboratories, 162–0112), and nonspecific binding sites were blocked by treating with 5% non-fat dry milk (Fisher Scientific, NC0339922) or Licor blocking buffer (Li-Cor Biosciences, 927–40000). The membranes were then incubated with primary antibodies directed against LC3 (1:1000), ATG7 (1:1000) or ATG9 (1:1000). The primary antibody treatments were followed by treatment with an HRP-conjugated secondary antibody (for the ECL detection system) or secondary IR dye-800 conjugated anti-rabbit dye or Alexa Fluor 680 conjugated anti-mouse IgG (for the Licor Odyssey system) for 1 h at room temperature. To confirm equal protein loading, blots were reprobed with anti-ACTB antibody (1:5000 dilution) or α-tubulin antibody (1:5000 dilution). For band detection, the membranes were incubated with a western blot detection system (ECL Plus) and exposed to single-emulsion film (Biomax MR Sigma, Z370398–50EA). Band intensities were determined using software developed by Wayne Rasband (ImageJ; National Institutes of Health, Bethesda, MD; available at http://rsb.info.nih.gov/ij/index.html). Statistical significance was calculated using the Mann-Whitney U-test.

Human donor retina

Human eyes were obtained from deceased and de-identified AMD patient and age-matched non-AMD control donors from the Lions Eye Bank of Oregon and NDRI with full approval for use in research. Four eyes from each age-group (young, old, early AMD and late AMD) were used.

AMD mouse models

Human apolipoprotein E4 targeted-replacement (*APOE4*) mice at the age of 14–15 mo were fed with a high fat, cholesterol-enriched (HFC) diet for a period of 2 mo.[24] Age-matched *APOE4* mice maintained on a normal diet (ND) throughout were treated as a control group (n = 10) to compare to the *APOE4*-HFC mice (n = 10) for comparison of autophagic protein levels by protein gel blot. For immunohistochemistry 6 mice from each group were sacrificed and probed with respective antibodies.

The SOD2 knockdown model was based on the AMD model as described by Justilien et al.[23] Briefly 6-wk-old mice received subretinal injection with AAV1-Rz-*Sod2* construct in one eye and AAV1 expressing inactive ribozyme in the contralateral eye. The mice were sacrificed at 1, 3, and 6 mo post injection and the retinas were analyzed for expression of autophagic proteins by immunohistochemistry.

Perfusion and dissection of mouse eyes

The mice were euthanized using CO_2 and immediately perfused with phosphate-buffered saline (PBS; Cellgro, 10–040-CV) before one eye was enucleated and kept on ice. Then the mouse was further perfused with 4% paraformaldehyde before the second eye was removed for immunohistochemistry. The cornea, lens, retina, and connective tissue were quickly removed from the PBS-perfused eye and the RPE/choroid/sclera was immediately frozen. Lysates were made for subsequent biochemistry analysis as follows: 80 μl of RIPA buffer with protease inhibitors was added to each tube containing each RPE/choroid/sclera, and the tissue was homogenized with a micro grinder (Argos). After sitting on ice for 30 min with vortexing every 10 min the samples were centrifuged at 8,000 g for 15 min and the supernatant fraction removed. The protein concentration was measured using a BCA protein assay kit (Pierce, 23227).

Autophagosome detection by immunostaining

After completion of respective treatments cells were washed 2 times in PBS and fixed in 4% paraformaldehyde for 15 min and subsequently immunostained with rabbit polyclonal LC3 antibody (Novus Biologicals, NB100–2220) for autophagic puncta. Fluorescent micrographs of immunostained LC3 were obtained and analyzed by Axiovision Rel 4.4 software (Zeiss, Oberkochen, Germany). The punctate staining of LC3 formed after oxidative stress indicated the formation of autophagosomes.

Assay for reactive oxygen species (ROS)

Cells were harvested and incubated in PBS containing 10 μM CM-H2DCFDA (the chloromethyl derivative of 2′,7′-dichlorodihydrofluorescein diacetate; Life Technologies, D-399) for 30 min at 37°C in the dark to allow loading of dye into the cells. This dye is nonfluorescent when chemically reduced, but after cellular oxidation and removal of acetate groups by cellular esterases it becomes fluorescent. The intracellular production of ROS was monitored by flow cytometer with excitation at 480 nm and emission at 530 nm.

Protein carbonyl assay

Protein carbonyl levels in ARPE-19 cells after treatment with H_2O_2 were measured spectrophotometrically using a commercial kit according to instructions (Cayman Chemical company, 10005020) using a 96-well format. Briefly, ARPE-19 cells grown

on 75-cm² flasks were treated with varying concentrations of H_2O_2 for indicated time-points and were scraped and collected by centrifugation at $2000 \times g$ for 10 min at 4°C. A bovine serum standard curve was created according to the kit instructions to assess the level of protein samples. The protein content in the samples was calculated based on A280 nm on a NanoDropTM spectrophotometer and carbonyl content was determined in the final pellets [(carbonyl nmol/ml)/ (protein mg/ml)].

Assessment of mitochondrial membrane potential by JC-1 dye

Following incubation of cells on either clear-bottom black 96-well tissue culture plates (BD Biosciences, 354649) or 8-well glass chamber slides (Nunc ®, C7057), cells were loaded with JC-1 dye (5 μg/ml) for 10 min at 37°C. Following incubation, the plates were centrifuged at $400 \times g$ at room temperature and the cells were washed gently, 3 times, in PBS (1×) and fixed in 4% paraformaldehyde solution for 15 min in the dark at room temperature. Dye distribution was analyzed on a Biotek® Fluorescence Microplate Reader. JC-1 aggregates (red) have an excitation/emission spectra of (560/595 nm) and monomer JC-1 has an excitation/emission spectra of (485/535 nm). The fluorescence values of each channel, and each well were recorded and red/green ratio was calculated as an indicator of mitochondrial membrane potential. Red/green ratio values positively correlate with mitochondrial membrane potential. In the case of the chamber slides, they were washed once with PBS (1×) following fixation and immediately mounted on coverslips and photographed on a Zeiss LSM 710 confocal microscope.

Estimation of mitochondrial mass

After respective treatments, ARPE-19 cells were loaded with MitoTracker Green dye (Excitation/Emission: 490/516 nm) at 100 nM final concentration (37°C for 15 min). Cells were washed with PBS and collected after trypsinization with 0.05% trypsin. 10,000 cells per treatment were analyzed using a BD LSR II® flow cytometer for MitoTracker fluorescence intensity.

Glutathione assay

Intracellular GSH:GSSG ratio was measured using a glutathione assay kit (Cayman Chemical Co, 703002) following the manufacturer's guidelines. Briefly, ARPE-19 cells were scraped off the wells after the incubation period, washed in PBS and centrifuged at $1000 \times g$ at 4°C. The pellet fraction was lysed and briefly sonicated followed by deproteination with metaphosphoric acid (Sigma-Aldrich, 239275) and triethanolamine (Sigma Aldrich T58300). Equal volumes from each deproteinated sample was then analyzed for GSH and derivatized by 2-vinylpyridine, and measured for GSSG (Sigma Aldrich, 132292). Results are expressed as the ratio of intracellular GSH: GSSG.

Lentiviral knockdown of *BECN1* and *ATG7* in ARPE-19 cells

The *BECN1* (Open Biosystems, RHS4533-EG8678, clone IDs: TRCN0000033549, TRCN0000033550, TRCN00

033551, TRCN0000033552, TRCN0000033553) and *ATG7* (Open Biosystems, RHS4533-EG10533, clone IDs: TRCN0000007585, TRCN0000007586, TRCN0000007587, TRCN0000007588) human lentiviral shRNA constructs were obtained and used according to the manufacturer's instructions. Since these constructs are all in the pLKO.1 puromycin vector (Addgene, 8453), a scrambled sequence with no sequence homology to the mammalian genome cloned into pLKO.1 vector was obtained (Addgene, 1864). Scrambled, *BECN1* or *ATG7* shRNA-encoding lentiviral vectors were transfected into HEK293T cells together with lentiviral packaging plasmids psPAX2 (Addgene, 12260) and pMD2.G (Addgene 12259), using Lipofectamine 2000, following the manufacturer's instructions (*BECN1* Clone 1: TRCN0000033549, TRCN0000033550, TRCN0000033551 and Clone 2: TRCN0000033552, TRCN0000033553; ATG7 Clone 1: TRCN0000007585, TRCN0000007586, and Clone 2: TRCN0000007587, TRCN0000007588). Culture supernatant fraction containing pseudovirus was collected 24, 48, and 72 h after transfection, mixed with polybrene, and filtered to create each viral titer. ARPE-19 cells grown on 25-cm2 flasks were transduced with each viral titer and 48 h later the cells were subjected to 2 μg/ml puromycin-selection medium. A further, 48 h later the clones were further passaged and assessed for protein expression by western blot.

Photoreceptor outer segment isolation

Photoreceptor outer segments (POS) were isolated and purified from light-adapted bovine retinas as previously described.[57] Isolated ROS were suspended in culture medium to give a final concentration of 2×10^7 POS/ml.

Analysis of lipofuscin accumulation in cultured RPE cells

Lipofuscin levels in cultured RPE cells were quantified by fluorescence-activated cell sorting (FACS) as described previously.[22] Briefly, after treatment RPE cells were harvested and resuspended in PBS at 1×10^5 cells/ml. The mean autofluorescence was measured by FACS, with an excitation at 488 nm and emission at 600 nm. Accumulation was also assessed by fluorescence microscopy.

MTT assay for mitochondrial respiration

The 3-(4, 5-dimethylthiazol-3-yl)-2,5-diphenyl tetrazolium bromide (MTT) assay was used to assess mitochondrial activity. Cells were washed once and then incubated with 0.25 mg/ml MTT in serum-free medium at 37°C for 3 h. The medium was then removed and dimethylsulfoxide was added to solubilize the produced blue formazan (MTT metabolic product). The density of blue formazan was measured at 570 nm with a reference wavelength at 630 nm using a microplate reader.

Crystal violet cell viability assay

The relative cell number was determined by crystal violet uptake as previously described.[58] Cells were washed 3 times in PBS, fixed in 4% paraformaldehyde in PBS and stained in a solution of 0.1% crystal violet (Sigma Aldrich, C-3866), 10%

ethanol. After washing 3 times in PBS, the remaining stain was dissolved in 10% acetic acid and absorbance measured with a microplate reader at 540 nm.

Immunohistochemistry

Human and mouse eyes were processed for standard paraffin embedding. Sections of 4-μm thickness from the same retinal region (human central retina outside the macula and mouse nasal quadrant) were cut and air-dried. The sections were deparaffinized/rehydrated in xylene and serial concentrations of ethanol. Antigen unmasking was achieved with Diva (Biocare Medical, DV2004 LX) or Rodent Decloaker (Biocare Medical, RD913), blocked with 5% normal goat serum (Invitrogen, PCN5000) and 1% BSA (Fisher Scientific, 50–176–714) for 1 h at room temperature, and probed with respective primary antibodies overnight at 4°C. After primary incubation, the specimens were washed with PBS and probed with fluorochrome-conjugated secondary antibody (Alexa Fluor 488, Invitrogen, A-11008; Alexa Fluor 594, Invitrogen, A-11005). On completion of washes after secondary incubation, the specimen sections were covered with Vectashield mounting medium with DAPI (Vector Lab, H-1200).

Electron microscopy

Briefly, eyes without lens and cornea were fixed in 2.5% paraformaldehyde (Pierce 28908) and 2.5% glutaraldehyde (Fisher Scientific, BP2547–1) in 0.125 M cacodylate buffer (pH 7.4) (Fisher Scientific, 50–980–232) with 2 mM $CaCl_2$. Upon postfixing with 2% osmium tetroxide in 0.1 M cacodylate buffer (pH 7.4) and en bloc staining with uranyl acetate (Sigma Aldrich, 73943), the tissue was dehydrated through a graded ethanol series and embedded in PolyBed 812 (Polysciences, 08792–1). Thin sections (60 nm) were examined on a JEOL 100CX transmission electron microscope.

Measurement of autophagic fractional volume

In double-blind experiments, 10 to 12 images of retinal RPEs per eye were taken at 4000× magnification using a JEOL 100CX electron microscope. The negatives were digitally scanned and inverted using an Epson 4990 photo scanner, then visualized using ImageJ software. A scale was set to micrometers and a point grid (0.5 μm^2/point) was superimposed over the image. Autophagic vacuoles were identified by their distinct double-membrane ultrastructure, and the number of points overlapping the autophagic vacuoles counted. The data are expressed as a fractional volume by comparing to the number of points that overlapped the RPE cytoplasm (minus nucleus).[59-61]

Data analysis

The results are expressed as the means ± SEM. Data analysis was performed using Prism 5.0 software (GraphPad Software, San Diego, CA). Data were analyzed using the Student t test, one-way ANOVA for multiple comparisons or the Mann-Whitney U test as appropriate. Differences with $P < 0.05$ were considered statistically significant.

Disclosure of Potential Conflicts of Interest

No potential conflicts of interest were disclosed.

References

1. Choi AM, Ryter SW, Levine B. Autophagy in human health and disease. N Engl J Med 2013; 368:1845-6; PMID:23656658; http://dx.doi.org/10.1056/NEJMra1205406

2. Sridhar S, Botbol Y, Macian F, Cuervo AM. Autophagy and disease: always two sides to a problem. J Pathol 2012; 226:255-73; PMID:21990109; http://dx.doi.org/10.1002/path.3025

3. Cuervo AM, Wong E. Chaperone-mediated autophagy: roles in disease and aging. Cell Res 2014; 24:92-104; PMID:24281265

4. Park C, Cuervo AM. Selective autophagy: talking with the UPS. Cell Biochem Biophys 2013; 67:3-13; PMID:23709310; http://dx.doi.org/10.1007/s12013-013-9623-7

5. Seo SJ, Krebs MP, Mao H, Jones K, Conners M, Lewin AS. Pathological consequences of long-term mitochondrial oxidative stress in the mouse retinal pigment epithelium. Exp Eye Res 2012; 101:60-71; PMID:22687918; http://dx.doi.org/10.1016/j.exer.2012.05.013

6. Lee J, Giordano S, Zhang J. Autophagy, mitochondria and oxidative stress: cross-talk and redox signalling. Biochem J 2012; 441:523-40; PMID:22187934; http://dx.doi.org/10.1042/BJ20111451

7. Kaarniranta K, Sinha D, Blasiak J, Kauppinen A, Vereb Z, Salminen A, Boulton ME, Petrovski G. Autophagy and heterophagy dysregulation leads to retinal pigment epithelium dysfunction and development of age-related macular degeneration. Autophagy 2013; 9:973-84; PMID:23590900; http://dx.doi.org/10.4161/auto.24546

8. Rami A. Review: autophagy in neurodegeneration: firefighter and/or incendiarist? Neuropathol Appl Neurobiol 2009; 35:449-61; PMID:19555462; http://dx.doi.org/10.1111/j.1365-2990.2009.01034.x

9. Wong E, Cuervo AM. Autophagy gone awry in neurodegenerative diseases. Nat Neurosci 2010; 13:805-11; PMID:20581817; http://dx.doi.org/10.1038/nn.2575

10. Boulton ME. Aging of the retina and retinal pigment epithelium. In: Holz F, Pauleikhoff D, Spade R, Bird A, eds. Age-Related Macular Degeneration. Berlin, Heidelberg: Springer Verlag, 2011:45-64.

11. Jarrett SG, Boulton ME. Consequences of oxidative stress in age-related macular degeneration. Mol Aspects Med 2012; 33:399-417; PMID:22510306; http://dx.doi.org/10.1016/j.mam.2012.03.009

12. Karunadharma PP, Nordgaard CL, Olsen TW, Ferrington DA. Mitochondrial DNA damage as a potential mechanism for age-related macular degeneration. Investigat Ophthalmol Visual Sci 2010; 51:5470-9; PMID:20505194; http://dx.doi.org/10.1167/iovs.10-5429

13. Kim JY, Zhao H, Martinez J, Doggett TA, Kolesnikov AV, Tang PH, Ablonczy Z, Chan CC, Zhou Z, Green DR, et al. Noncanonical autophagy promotes the visual cycle. Cell 2013; 154:365-76; PMID:23870125; http://dx.doi.org/10.1016/j.cell.2013.06.012

14. Mitter SK, Rao HV, Qi X, Cai J, Sugrue A, Dunn WA Jr, Grant MB, Boulton ME. Autophagy in the retina: a potential role in age-related macular degeneration. Adv Exp Med Biol 2012; 723:83-90; PMID:22183319; http://dx.doi.org/10.1007/978-1-4614-0631-0_12

15. Ryhanen T, Hyttinen JM, Kopitz J, Rilla K, Kuusisto E, Mannermaa E, Viiri J, Holmberg CI, Immonen I, Meri S, et al. Crosstalk between Hsp70 molecular chaperone, lysosomes and proteasomes in autophagy-mediated proteolysis in human retinal pigment epithelial cells. J Cell Mol Med 2009; 13:3616-31; PMID:19017362; http://dx.doi.org/10.1111/j.1582-4934.2008.00577.x

16. Yoon YH, Cho KS, Hwang JJ, Lee SJ, Choi JA, Koh JY. Induction of lysosomal dilatation, arrested autophagy, and cell death by chloroquine in cultured ARPE-19 cells. Invest Ophthalmol Visual Sci 2010; 51:6030-7; PMID:20574031; http://dx.doi.org/10.1167/iovs.10-5278

17. Boulton ME. Lipofuscin of the RPE. In: Lois N, Forrester J, eds. Fundus Autofluorescence: Lippincott, Williams and Wilkins, 2009:14-26.

18. Wang AL, Boulton ME, Dunn WA Jr, Rao HV, Cai J, Lukas TJ, Neufeld AH. Using LC3 to monitor autophagy flux in the retinal pigment epithelium. Autophagy 2009; 5:1190-3; PMID:19855195; http://dx.doi.org/10.4161/auto.5.8.10087

19. Ayala A, Venero JL, Cano J, Machado A. Mitochondrial toxins and neurodegenerative diseases. Front Biosci 2007; 12:986-1007; PMID:17127354; http://dx.doi.org/10.2741/2119

20. Dasuri K, Zhang L, Keller JN. Oxidative stress, neurodegeneration, and the balance of protein degradation and protein synthesis. Free Radic Biol Med 2013; 62:170-85; PMID:23000246; http://dx.doi.org/10.1016/j.freeradbiomed.2012.09.016

21. Flynn JM, Melov S. SOD2 in mitochondrial dysfunction and neurodegeneration. Free Radic Biol Med 2013; 62:4-12; PMID:23727323; http://dx.doi.org/10.1016/j.freeradbiomed.2013.05.027

22. Thampi P, Rao HV, Mitter SK, Cai J, Mao H, Li H, Seo S, Qi X, Lewin AS, Romano C, et al. The 5HT1a receptor agonist 8-Oh DPAT induces protection from lipofuscin accumulation and oxidative stress in the retinal pigment epithelium. PLoS One 2012; 7:e34468; PMID:22509307; http://dx.doi.org/10.1371/journal.pone.0034468

23. Justilien V, Pang JJ, Renganathan K, Zhan X, Crabb JW, Kim SR, Sparrow JR, Hauswirth WW, Lewin AS. SOD2 knockdown mouse model of early AMD. Invest Ophthalmol Visual Sci 2007; 48:4407-20; PMID:17898259; http://dx.doi.org/10.1167/iovs.07-0432

24. Malek G, Johnson LV, Mace BE, Saloupis P, Schmechel DE, Rickman DW, Toth CA, Sullivan PM, Bowes Rickman C. Apolipoprotein E allele-dependent pathogenesis: a model for age-related retinal degeneration. Proc Natl Acad Sci U S A 2005; 102:11900-5; PMID:16079201; http://dx.doi.org/10.1073/pnas.0503015102

25. Chen Y, Sawada O, Kohno H, Le YZ, Subauste C, Maeda T, Maeda A. Autophagy protects the retina from light-induced degeneration. J Biol Chem 2013; 288:7506-18; PMID:23341467; http://dx.doi.org/10.1074/jbc.M112.439935

26. Suzuki M, Tsujikawa M, Itabe H, Du ZJ, Xie P, Matsumura N, Fu X, Zhang R, Sonoda KH, Egashira K, et al. Chronic photo-oxidative stress and subsequent MCP-1 activation as causative factors for age-related macular degeneration. J Cell Sci 2012; 125:2407-15; PMID:22357958; http://dx.doi.org/10.1242/jcs.097683

27. Munemasa Y, Kwong JM, Kim SH, Ahn JH, Caprioli J, Piri N. Thioredoxins 1 and 2 protect retinal ganglion cells from pharmacologically induced oxidative stress, optic nerve transection and ocular hypertension. Adv Exp Med Biol 2010; 664:355-63; PMID:20238036; http://dx.doi.org/10.1007/978-1-4419-1399-9_41

28. Chen PM, Gombart ZJ, Chen JW. Chloroquine treatment of ARPE-19 cells leads to lysosome dilation and intracellular lipid accumulation: possible implications of lysosomal dysfunction in macular degeneration. Cell Biosci 2011; 1:10; PMID:21711726; http://dx.doi.org/10.1186/2045-3701-1-10

29. Krohne TU, Stratmann NK, Kopitz J, Holz FG. Effects of lipid peroxidation products on lipofuscinogenesis and autophagy in human retinal pigment epithelial cells. Exp Eye Res 2010; 90:465-71; PMID:20059996; http://dx.doi.org/10.1016/j.exer.2009.12.011

30. Viiri J, Amadio M, Marchesi N, Hyttinen JM, Kivinen N, Sironen R, Rilla K, Akhtar S, Provenzani A, D'Agostino VG, et al. Autophagy activation clears ELAVL1/HuR-mediated accumulation of SQSTM1/p62 during proteasomal inhibition in human retinal pigment epithelial cells. PloS One 2013; 8:e69563; PMID:23922739; http://dx.doi.org/10.1371/journal.pone.0069563

31. Wang AL, Lukas TJ, Yuan M, Du N, Tso MO, Neufeld AH. Autophagy, exosomes and drusen formation in age-related macular degeneration. Autophagy 2009; 5:563-4; PMID:19270489; http://dx.doi.org/10.4161/auto.5.4.8163

32. McCray BA, Taylor JP. The role of autophagy in age-related neurodegeneration. Neurosignals 2008; 16:75-84; PMID:18097162; http://dx.doi.org/10.1159/000109761

33. Singh R, Cuervo AM. Lipophagy: connecting autophagy and lipid metabolism. Int J Cell Biol 2012; 2012:282041; PMID:22536247; http://dx.doi.org/10.1155/2012/282041

34. Singh R, Kaushik S, Wang Y, Xiang Y, Novak I, Komatsu M, Tanaka K, Cuervo AM, Czaja MJ. Autophagy regulates lipid metabolism. Nature 2009; 458:1131-5; PMID:19339967; http://dx.doi.org/10.1038/nature07976

35. Lionaki E, Markaki M, Tavernarakis N. Autophagy and ageing: insights from invertebrate model organisms. Ageing Res Rev 2013; 12:413-28; PMID:22634332; http://dx.doi.org/10.1016/j.arr.2012.05.001

36. Beatty S, Koh H, Phil M, Henson D, Boulton M. The role of oxidative stress in the pathogenesis of age-related macular degeneration. Sur Ophthalmol 2000; 45:115-34; PMID:11033038; http://dx.doi.org/10.1016/S0039-6257(00)00140-5

37. Haque R, Chun E, Howell JC, Sengupta T, Chen D, Kim H. MicroRNA-30b-mediated regulation of catalase expression in human ARPE-19 cells. PLoS One 2012; 7:e42542; PMID:22900025; http://dx.doi.org/10.1371/journal.pone.0042542

38. Floor E, Wetzel MG. Increased protein oxidation in human substantia nigra pars compacta in comparison with basal ganglia and prefrontal cortex measured with an improved dinitrophenylhydrazine assay. J Neurochem 1998; 70:268-75; PMID:9422371; http://dx.doi.org/10.1046/j.1471-4159.1998.70010268.x

39. Hanus J, Zhang H, Wang Z, Liu Q, Zhou Q, Wang S. Induction of necrotic cell death by oxidative stress in retinal pigment epithelial cells. Cell Death Dis 2013; 4:e965; PMID:24336085; http://dx.doi.org/10.1038/cddis.2013.478

40. Kurz T, Karlsson M, Brunk UT, Nilsson SE, Frennesson C. ARPE-19 retinal pigment epithelial cells are highly resistant to oxidative stress and exercise strict control over their lysosomal redox-active iron. Autophagy 2009; 5:494-501; PMID:19223767; http://dx.doi.org/10.4161/auto.5.4.7961

41. Garg TK, Chang JY. Oxidative stress causes ERK phosphorylation and cell death in cultured retinal pigment epithelium: prevention of cell death by AG126 and 15-deoxy-delta 12, 14-PGJ2. BMC Ophthalmol 2003; 3:5; PMID:12659653; http://dx.doi.org/10.1186/1471-2415-3-5

42. Jarrett SG, Boulton ME. Antioxidant up-regulation and increased nuclear DNA protection play key roles in adaptation to oxidative stress in epithelial cells. Free Radic Biol Med 2005; 38:1382-91; PMID:15855056; http://dx.doi.org/10.1016/j.freeradbiomed.2005.02.003

43. Jarrett SG, Boulton ME. Poly(ADP-ribose) polymerase offers protection against oxidative and alkylation damage to the nuclear and mitochondrial genomes of the retinal pigment epithelium. Ophthalmic Res 2007; 39:213-23; PMID:17596754; http://dx.doi.org/10.1159/000104683

44. Halliwell B, Clement MV, Long LH. Hydrogen peroxide in the human body. FEBS Lett 2000; 486:10-3; PMID:11108833; http://dx.doi.org/10.1016/S0014-5793(00)02197-9

45. Miceli MV, Liles MR, Newsome DA. Evaluation of oxidative processes in human pigment epithelial cells associated with retinal outer segment phagocytosis. Exp Cell Res 1994; 214:242-9; PMID:8082727; http://dx.doi.org/10.1006/excr.1994.1254

46. Rodriguez-Muela N, Koga H, Garcia-Ledo L, de la Villa P, de la Rosa EJ, Cuervo AM, Boya P. Balance between autophagic pathways preserves retinal homeostasis. Aging Cell 2013; 12:478-88; PMID:23521856; http://dx.doi.org/10.1111/acel.12072

47. Cao Y, Klionsky DJ. Physiological functions of Atg6/Beclin 1: a unique autophagy-related protein. Cell Res 2007; 17:839-49; PMID:17893711; http://dx.doi.org/10.1038/cr.2007.78

48. Tanida I, Ueno T, Kominami E. LC3 and Autophagy. Methods Mol Biol 2008; 445:77-88; PMID:18425443; http://dx.doi.org/10.1007/978-1-59745-157-4_4

49. He C, Klionsky DJ. Atg9 trafficking in autophagy-related pathways. Autophagy 2007; 3:271-4; PMID:17329962; http://dx.doi.org/10.4161/auto.3912

50. Galluzzi L, Morselli E, Vicencio JM, Kepp O, Joza N, Tajeddine N, Kroemer G. Life, death and burial: multifaceted impact of autophagy. Biochemical Soc Trans 2008; 36:786-90; PMID:18793137; http://dx.doi.org/10.1042/BST0360786

51. Galluzzi L, Vicencio JM, Kepp O, Tasdemir E, Maiuri MC, Kroemer G. To die or not to die: that is the autophagic question. Curr Mol Med 2008; 8:78-91; PMID:18336289; http://dx.doi.org/10.2174/156652408783769616

52. Gozuacik D, Kimchi A. Autophagy and cell death. Curr Top Dev Biol 2007; 78:217-45; PMID:17338918; http://dx.doi.org/10.1016/S0070-2153(06)78006-1

53. Wong M. Mammalian target of rapamycin (mTOR) pathways in neurological diseases. Biomed J 2013; 36:40-50; PMID:23644232; http://dx.doi.org/10.4103/2319-4170.110365

54. Brunk UT, Terman A. The mitochondrial-lysosomal axis theory of aging: accumulation of damaged mitochondria as a result of imperfect autophagocytosis. Eur J Biochem 2002; 269:1996-2002; PMID:11985575; http://dx.doi.org/10.1046/j.1432-1033.2002.02869.x

55. Stroikin Y, Dalen H, Loof S, Terman A. Inhibition of autophagy with 3-methyladenine results in impaired turnover of lysosomes and accumulation of lipofuscin-like material. Eur J Cell Biol 2004; 83:583-90; PMID:15679103; http://dx.doi.org/10.1078/0171-9335-00433

56. Boulton ME, Marshall J, Mellerio J. Retinitis pigmentosa: a preliminary report on tissue culture studies of retinal pigment epithelial cells from eight affected human eyes. Exp Eye Res 1983; 37:307-13; PMID:6628578; http://dx.doi.org/10.1016/0014-4835(83)90166-5

57. Wassell J, Boulton M. A role for vitamin A in the formation of ocular lipofuscin. Br J Ophthalmol 1997; 81:911-8; PMID:9486037; http://dx.doi.org/10.1136/bjo.81.10.911

58. Cai J, Qi X, Kociok N, Skosyrski S, Emilio A, Ruan Q, Han S, Liu L, Chen Z, Bowes Rickman C. beta-Secretase (BACE1) inhibition causes retinal pathology by vascular dysregulation and accumulation of age pigment. EMBO Mol Med 2012; 4:980-91; PMID:22903875; http://dx.doi.org/10.1002/emmm.201101084

59. Dunn WA Jr. Studies on the mechanisms of autophagy: formation of the autophagic vacuole. J Cell Biol 1990; 110:1923-33; PMID:2351689; http://dx.doi.org/10.1083/jcb.110.6.1923

60. Dunn WA Jr. Studies on the mechanisms of autophagy: maturation of the autophagic vacuole. J Cell Biol 1990; 110:1935-45; PMID:2161853; http://dx.doi.org/10.1083/jcb.110.6.1935

61. Weibel ER, Staubli W, Gnagi HR, Hess FA. Correlated morphometric and biochemical studies on the liver cell. I. Morphometric model, stereologic methods, and normal morphometric data for rat liver. J Cell Biol 1969; 42:68-91; PMID:4891915; http://dx.doi.org/10.1083/jcb.42.1.68